

6-2022

**EFFECTS OF WETTABILITY, LITHOLOGY, AND PERMEABILITY ON  
THE OPTIMUM SLUG SIZE OF LOW SALINITY WATER FLOODING  
IN CARBONATES: AN EXPERIMENTAL APPROACH**

Hala Khaled Hasan Alshadafan

Follow this and additional works at: [https://scholarworks.uaeu.ac.ae/all\\_theses](https://scholarworks.uaeu.ac.ae/all_theses)



Part of the [Petroleum Engineering Commons](#)

---



MASTER THESIS NO. 2022: 42

College of Engineering

Department of Chemical and Petroleum Engineering

**EFFECTS OF WETTABILITY, LITHOLOGY, AND  
PERMEABILITY ON THE OPTIMUM SLUG SIZE OF LOW  
SALINITY WATER FLOODING IN CARBONATES: AN  
EXPERIMENTAL APPROACH**

*Hala Khaled Hasan Alshadafan*



*June 2022*

United Arab Emirates University

College of Engineering

Department of Chemical and Petroleum Engineering

EFFECTS OF WETTABILITY, LITHOLOGY, AND  
PERMEABILITY ON THE OPTIMUM SLUG SIZE OF  
LOW SALINITY WATER FLOODING IN  
CARBONATES: AN EXPERIMENTAL APPROACH

Hala Khaled Hasan Alshadafan

This thesis is submitted in partial fulfilment of the requirements for the  
degree of Master of Science in Petroleum Engineering

June 2022

**United Arab Emirates University Master Thesis  
2022: 42**

Cover: Image related to synthetic preparation of formation brine and seawater.

(Photo: By Hala Khaled Hasan Alshadafan)

© 2022 Copyright Hala Khaled Hasan Alshadafan, Al Ain, UAE  
All Rights Reserved

Print: University Print Service, UAEU 2022

## **Declaration of Original Work**




I, Hala Khaled Hasan Alshadafan, the undersigned, a graduate student at the United Arab Emirates University (UAEU), and the author of this thesis entitled “*Effects of Wettability, Lithology, and Permeability on the Optimum Slug Size of Low Salinity Water Flooding in Carbonates: An Experimental Approach*”, hereby, solemnly declare that this is the original research work done by me under the supervision of Professor Abdulrazag Zekri, in the College of Engineering at UAEU. This work has not previously formed the basis for the award of any academic degree, diploma or a similar title at this or any other university. Any materials borrowed from other sources (whether published or unpublished) and relied upon or included in my thesis have been properly cited and acknowledged in accordance with appropriate academic conventions. I further declare that there is no potential conflict of interest with respect to the research, data collection, authorship, presentation and/or publication of this thesis.

Student’s Signature: Hala Khaled Hasan Alshadafan

Date: 10<sup>th</sup> April 2022

## Approval of the Master Thesis

This Master Thesis is approved by the following Examining Committee Members:

- 1) Advisor (Committee Chair): Abdulrazag Zekri  
Title: Professor  
Department of Chemical and Petroleum Engineering  
College of Engineering  
  
Signature  Date: 6/10/2022
- 2) Member: Jinyu Tang  
Title: Assistant Professor  
Department of Chemical and Petroleum Engineering  
College of Engineering  
  
Signature  Date: 6/10/2022
- 3) Member (External Examiner): Denis José Schiozer  
Title: Professor  
Department of Energi Simulation  
Institution: University of Campinas, UNICAMP, Brazil  
  
Signature  Date: 6/4/2022

This Master Thesis is accepted by:

Acting Dean of the College of Engineering: Professor Mohamed Al-Marzouqi

Signature Mohamed AlMarzouqi

Date August 07, 2022

Dean of the College of Graduate Studies: Professor Ali Al-Marzouqi

Signature Ali Hassan

Date August 11, 2022

## Abstract

Low salinity water flooding has attracted the academic and industry communities due to its relatively simple and applicable technology. One of the drawbacks of applying IOR/EOR technique is the lack of the availability of the low salinity water in large quantities at reasonable cost required for a technically and environmentally successful project. To overcome this problem, the industry proposed to use produced water/sea water after dilution, and reverse osmosis filter technology to achieve the required salinity. Both techniques are quite costly and might hinder the project economic success. A low salinity water as slug size followed by high salinity water was proposed to reduce the project requirement of sweet water and make the project technically and economically more attractive. In this project, the effect of the carbonate reservoir wettability, reservoir lithology (limestone and dolomite), and permeability (low and high) on the design of low salinity slug injection have been investigated. Oil wet and water wet high permeability limestone cores and high and low permeability oil wet dolomites cores were flooded in a secondary mode by the following low salinity slug sizes 10, 20, 30, and 40% of pore volumes followed by continuous flooding with high salinity water until reaching stable value of 100% water cut. Results indicated that in the case of limestone environment, wettability of the reservoir has a significant impact on the optimum LSW slug size and a lower slug size requirement was observed in the case of oil wet system 10% PV as compared to 30% PV for water wet system. In addition to the that, 90% of the oil in place was recovered as compared to 60% OIP for the water wet system. The lithology of the system had no noticeable impact on the requirement for the slug size in oil wet environment. Low salinity flooding required relatively a smaller slug size in a high permeability environment for the dolomite oil wet system, while low



permeability system exhibited a higher oil recovery as compared to high permeability environment. Therefore, in performing a reservoir simulation of low salinity flooding of a mixed wettability and heterogenous system, a laboratory work is recommended using reservoir rock and fluid data to the determine optimum slug size and relative permeability data.

**Keywords:** Low salinity water, Limestone, Dolomite, Slug, Permeability, Wettability, Lithology.

## Title and Abstract (in Arabic)

آثار القابلية للرطوبة، والليثولوجيا، والقدرة على النفاذية على الحجم الأمثل لمياه منخفضة  
الملوحة في الفيضانات في الكربونات

### الملخص

اجتذبت طريقة حقن المياه منخفضة الملوحة الأوساط الأكاديمية والصناعية وذلك لسهولة وقابلية تنفيذ هذه التقنية في معظم المكامن الكربونية. تتمثل إحدى عيوب تطبيق هذه التقنية في عدم توفر المياه منخفضة الملوحة بكميات كبيرة بتكلفة معقولة مطلوبة لمشروع ناجح تقنياً وبيئياً. للتغلب على هذه المشكلة، اقترحت الصناعة استخدام المياه المنتجة / مياه البحر بعد التخفيف أو استخدام تقنية الترشيح بالتناضح العكسي لتحقيق الملوحة المطلوبة. كلتا الطريقتين مكلفتين للغاية وقد تعوقان النجاح الاقتصادي للمشروع. تم اقتراح حقن كمية محددة من المياه منخفضة الملوحة متبوعة بمياه عالية الملوحة لتقليل متطلبات المشروع من المياه العذبة وجعل المشروع أكثر جاذبية من الناحية الفنية والاقتصادية. في هذا المشروع، تم دراسة تأثير رطوبة المكامن الكربونية وصخور الخزان (الحجر الجيري والدولوميت)، والنفاذية (منخفضة وعالية) على تصميم حقن الجزي للمياه منخفضة الملوحة. حيث تم حقن عينات من الصخر الجيري والدولمايت ذات النفاذية والرطوبة المختلفة بكميات من المياه منخفضة الملوحة التالية 10 و20 و30 و40% من أحجام المسام، متبوعة بالفيضانات المستمر للمياه ذات الملوحة العالية. أشارت النتائج إلى أنه في حالة الحجر الجيري، فرطوبة المكامن لها تأثير كبير على الحجم المثالي المطلوب للحقن. كما دلت نتائج هذا البحث على أن للنفاذية تأثير عكسي بالنسبة للحجم المثالي ومعدل الاستخراج الكلي للحقن.

مفاهيم البحث الرئيسية: مياه منخفضة الملوحة، حجر جيري، دولوميت، فيضان متقطع، نفاذية، قابلية رطوبة، صخور.

## **Author Profile**

Hala K. Alshadafan graduated with honors from UAEU Chemical & Petroleum Engineering Department, earning a bachelor's degree in Petroleum Engineering in June of 2020. As an undergraduate, Alshadafan and colleagues published a paper titled “Integrated Optimum Design of Hydraulic Fracturing for Tight Hydrocarbon-bearing Reservoirs” in the Journal of Petroleum Exploration and Production Technology. Hala K. Alshadafan decided to pursue higher education in engineering. In the Fall of 2020, the author received UAEU Chancellor's Fellowship Award for being an excelling woman in STEM. As an aspiring energy provider and enthusiastic researcher, Alshadafan worked on this thesis research hoping to provide clarity for a complex technical mechanism in the IOR field to help the industry meet growing energy demands.

The author advocates for energy diversification and transition to secure a more sustainable future by participating in transnational initiatives including Expo 2020: Swiss Middle East Circular Youth Initiative. Ventures of Alshadafan that reflect her innovative mindset include being selected to join the First Batch for the UAEU Innovation Disruptors & Entrepreneurship Journey. Working as a research assistant made the author conscious of the importance of effective health and safety awareness and management. This prompted the author to pursue certification by the National Examination Board in Occupational Safety and Health (NEBOSH) in Spring of 2022.

Dubai, UAE +971547895367

## **Acknowledgements**

I would like to thank my committee for their guidance, support, and assistance throughout the preparation of this thesis, especially my advisor Professor Abdulrazag Zekri and lab supervisor Dr Essa Georges Lwisa.

Special thanks go to my supportive family.

## Dedication

*To my beloved supportive father and beautiful mother.*

## Table of Contents

Title.....	i
Declaration of Original Work.....	iii
Approval of the Master Thesis .....	iv
Abstract.....	vi
Title and Abstract (in Arabic).....	viii
Author Profile.....	ix
Acknowledgements .....	x
Dedication.....	xi
Table of Contents .....	xii
List of Tables.....	xiv
List of Figures.....	xv
List of Abbreviations.....	xvi
Chapter 1: Introduction.....	3
1.1 Overview .....	3
1.2 Statement of the Problem .....	5
1.3 Research Objectives .....	6
1.4 Relevant Literature .....	7
Chapter 2: Methods .....	15
2.1 Research Design.....	15
2.2 Data Collection.....	17
2.2.1 Core Samples and Petrophysical Properties .....	17
2.2.2 Fluids .....	23
2.2.3 System Selection and Core Saturation.....	26
2.2.4 Oil Flooding.....	27
2.2.5 Improved Oil Recovery .....	33
2.2.6 Interfacial Tension (IFT) Measurement.....	40
2.2.7 Contact Angle Measurement .....	44
2.2.8 Effluent Analysis .....	47

Chapter 3: Results and Discussions.....	51
3.1 Overview of the Main Findings.....	51
Chapter 4: Conclusion .....	63
4.1 Managerial Implication.....	63
4.2 Research Implications.....	64
4.3 Future Endeavors.....	66
References .....	68
List of Publications.....	73

## List of Tables

Table 1: Limestone Group ZE-1 Average Dimensions and Petrophysical Properties.....	21
Table 2: Dolomite Group ZE-2 Average Dimensions and Petrophysical Properties.....	22
Table 3: Asab Brine Ion Content.....	23
Table 4: Composition of Asab Brine.....	24
Table 5: Seawater Ion Content.....	25
Table 6: Composition of Seawater.....	25
Table 7: Core Samples Classification for Limestone Group ZE-1 According to the Intended Investigation.....	26
Table 8: Core Samples Classification for Dolomite Group ZE-2 According to the Intended Investigation.....	27
Table 9: Oil-Wet Limestone Primary Oil Flood Results (ZE1).....	29
Table 10: Oil-Wet Dolomite Primary Oil Flood Results (ZE2).....	29
Table 11: Oil-Wet Limestone Secondary Oil Flood Results (ZE1).....	31
Table 12: Oil-Wet Dolomite Secondary Oil Flood Results (ZE2).....	32
Table 13: Water-Wet Limestone Samples Oil Flood Results (ZE1).....	32
Table 14: IOR Results of Water-Wet High-k Limestone Samples.....	34
Table 15: IOR Results of Oil-Wet High-k Limestone Samples.....	35
Table 16: IOR Results of Oil-Wet High-k Dolomite Samples.....	36
Table 17: IOR Results of Oil-Wet Low-k Dolomite Samples.....	37
Table 18: Summary of IFT Results for Asab Brine/Asab Crude System.....	41
Table 19: IFT Results for Asab Brine/Asab Crude System.....	41
Table 20: Summary of IFT Results for Low-Salinity SW/Asab Crude System.....	42
Table 21: IFT Results for Low-Salinity SW/Asab Crude System.....	43
Table 22: Measurement of Trim-Ends Contact Angle.....	46
Table 23: Effluent Analysis of Cations Concentration.....	48
Table 24: Post-IOR Average pH Readings.....	56
Table 25: Change in Petrophysical Properties After IOR.....	57
Table 26: Change in Crude Properties After IOR.....	58



## List of Figures

Figure 1: EIA Global Primary Energy Consumption (2019).....	4
Figure 2: EIA World Liquid Fuels Production and Consumption Forecast (2022).....	4
Figure 3: BP Statistical Forecast of Fuel Shares (2019).....	5
Figure 4: Stage 1 of Research Methodology .....	15
Figure 5: Stage 2 of Research Methodology .....	16
Figure 6: Soxhlet Extractor.....	18
Figure 7: Poroperm.....	19
Figure 8: Pycnometer and Weighing Balance .....	24
Figure 9: Brine Preparation Setup .....	24
Figure 10: Separability Test .....	28
Figure 11: Precipitate at Limestone Core-Head .....	29
Figure 12: Samples Aged in Brine .....	30
Figure 13: Samples Aged in Crude.....	30
Figure 14: Core Flooding Apparatus.....	31
Figure 15: Optimum Slug-Size of Water-Wet High-k Limestone Group .....	38
Figure 16: Optimum Slug-Size of Oil-Wet High-k Limestone Group .....	38
Figure 17: Optimum Slug-Size of Oil-Wet High-k Dolomite Group .....	39
Figure 18: Optimum Slug-Size of Oil-Wet Low-k Dolomite Group .....	39
Figure 19: KRUSS Spinning Drop Tensiometer .....	40
Figure 20: Oil Drop in Asab Brine .....	41
Figure 21: IFT Ascending Trend in Asab Brine.....	42
Figure 22: Oil Drop in Low-Salinity SW .....	43
Figure 23: IFT Descending Trend in Low-Salinity SW .....	44
Figure 24: Core Trimmer.....	45

## **List of Abbreviations**

FW	Formation Water
IFT	Interfacial Tension
IOR	Improved Oil Recovery
LSWF	Low Salinity Waterflood
MIE	Multicomponent Ionic Exchange
$N_c$	Capillary Number
OOIP	Original Oil in Place
PDI	Potential Determining Ions
PV	Pore Volume
RF	Recovery Factor
$S_{or}$	Residual Oil Saturation
SW	Seawater
SW/10	Diluted Seawater

# Chapter 1



# Chapter 1: Introduction

## 1.1 Overview

According to the 2019 predictions of the U.S. Energy Information Administration, hydrocarbons from conventional and unconventional reservoirs are most likely to remain the major contributor to the growing energy demand in the next 30 years (Figure 1). The global pandemic that started at the end of the same year however, introduced an unexpected dip (Figure 2) and generated new challenges to the industry. Forecasts made in February of 2022 by EIA displays that the world oil markets have successfully rebounded from the massive demand shock. Prices have risen due to current heightened market concerns about the possibility of oil supply disruptions, this is notably related to recent political tensions paired with receding market concerns about the Omicron variant of COVID-19 and its possible effects on oil consumption. Fluctuations influenced by global supply, demand, and geopolitics along with the fast-evolving governmental plans to accelerate transitions towards a more sustainable future in response to emotive public arguments against the industry creates a constant degree of market volatility.

Most hydrocarbon alternatives remain immature and not economically feasible, according to BP statistical review of world energy in 2019 (Figure 3), it will take until 2040 for renewables to produce more primary energy than coal and gas. Thus, despite governmental and public pressures, it is the hydrocarbon industry's responsibility to supply an abundance of low-cost energy to prevent the social disruption that would ensue if demand outstripped supply. This calls for recovery techniques designed to maximize hydrocarbon yield while minimizing operational

costs and environmental imprint. This thesis explores designer water in secondary mode which falls under improved oil recovery.

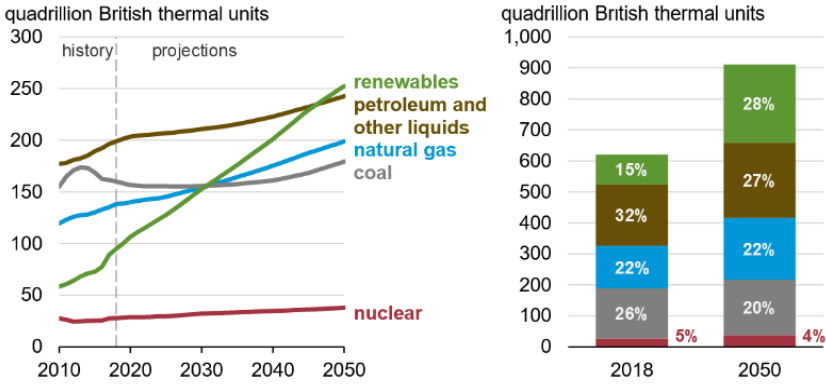


Figure 1: EIA Global Primary Energy Consumption (2019)

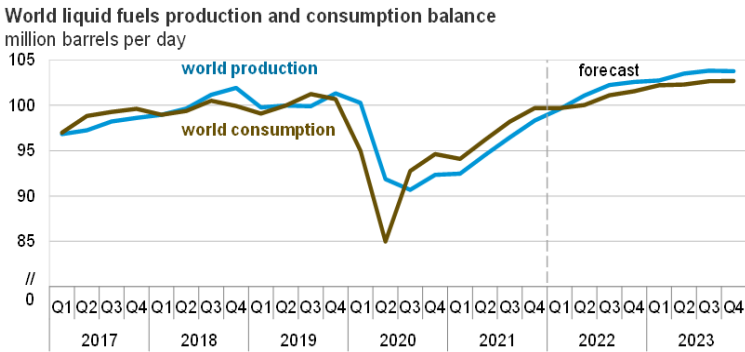


Figure 2: EIA World Liquid Fuels Production and Consumption Forecast (2022)

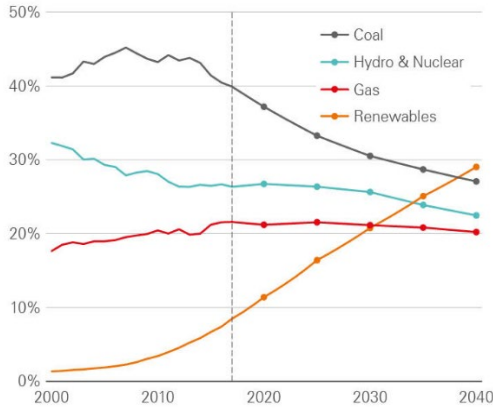


Figure 3: BP Statistical Forecast of Fuel Shares (2019)

## 1.2 Statement of the Problem

Designer water, also known as advanced ion management or smart waterflooding, is a technique in which engineers manipulate the ionic composition of the displacing phase. Flooding fluid destabilizes the initial equilibrium of the crude/brine/grain system which results in wettability alteration (Sheng, 2013). This field of study is attractive when compared to EOR processes because it's economically feasible (doesn't require expensive chemicals), allows use both at secondary mode (early stage of oil recovery) or tertiary mode (late life cycle of the reservoir), and environmentally friendly with no associated injection issues (Kazankapov, 2014). However, the principal mechanism of this technique demands much more research to detail it comprehensively.

The designed technique for this thesis operates as follows in secondary mode: a slug of low salinity diluted seawater is introduced at initial formation water saturation followed by the continuous flood by high salinity formation brine until 100% water cut is realized. This presents the

following curiosity, what percentage of effective Pore Volume (PV) to liquid should the low salinity slug be to yield maximum recovery and does wettability, lithology, and permeability affect this size.

### **1.3 Research Objectives**

Researchers agree that designer water improves displacement efficiency, i.e., increases the capillary number, however there is still debate on the mechanism especially in carbonate reservoirs. Capillary number is the dimensionless ratio of viscous forces to interfacial forces (Tiab & Donaldson, 2015). This parameter is optimized by either increasing the flow rate or lowering the interfacial tension, limitations in predicting turbulent flow behavior makes enhancing interfacial tension the more feasible option since it is a parameter that could be precisely controlled for a given system.

Experimental work on acquired limestone and dolomite samples will investigate the possibility of optimizing conventional designer water by introducing slugs and reducing the amount of diluted water required. This is critical in the Gulf region, where seawater salinity averages at about 50,000 ppm, its filtration is quite costly and might hinder the project's profitability. Measurement of Interfacial Tension (IFT) between flowing phases (Diluted seawater, Asab brine, and Asab crude), performance of effluent analysis pre and post IOR, measurement of the contact angle between the liquid interface and solid grain through the denser phase which is a function of the wetting characteristics of the matrix system and investigating changes in petrophysical properties of core will help justify findings and clarify mechanisms at work.

This thesis aims to define the optimum slug size during low salinity water flood for different lithology (Limestone/Dolomite),



wettability (oil wet/water wet), and permeability (high/low) environments through conducting experimental work.

#### **1.4 Relevant Literature**

Over the years, waterflooding proved to be one of the most popular hydrocarbon recovery methods. Researchers previously neglected the importance of salinity manipulation and its influence on the incremental recovery of hydrocarbons. Tang and Morrow (1997), along with latter researchers such as Webb et al. (2003) and McGuire et al. (2005), reported that low salinity water flooding is more effective in comparison to the contemporary recovery processes of high salinity water flooding due to its simplicity and potential benefits.

In the last decades, laboratory waterflood and successful field tests have proved improvement in oil recovery through the utilization of low salinity water flooding in sandstone reservoirs (Webb et al., 2003; McGuire et al., 2005; Zhang et al., 2006; Seccombe et al., 2008; Morrow & Buckley, 2011). This has earned LSWF technique popularity among oil companies and researchers due to its capability to efficiently displace hydrocarbons, additionally its application proved to reduce both scaling and souring (Erke et al., 2016).

Contrary to the observed recovery optimization in sandstones, the effect of salinity manipulation on carbonate formations, that are proved to contain more than half of the world's oil reserve (Akbar et al., 2001), has not shown significant growth due to the relatively limited experimental data, scarce reported cases of field-scale implementation, and lack of clear definition of this technique's leading mechanism.

Justifications of failed laboratory low salinity waterflood applications in carbonates varied. For example, Lager et al. (2008) argued that the absence of clays in most carbonates, which play a vital role in LSWF success in sandstones, explained such pessimistic results. While RezaeiDoust et al. (2009) clarified that such a lack in recovery improvement and contrasting results are to be expected considering the differing chemical mechanisms present in each formation, i.e., crude oil adsorption onto positively charged calcite surface and negatively charged quartz surface. In sandstones, low salinity brine was found to wash away cations bridging the negatively charged crude to the negatively charged clay. As a result, crude was repelled from clay surfaces and wettability was altered from oil-wet to water-wet, i.e., residual crude no longer existed as a film surrounding formation grains but rather droplets trapped by capillary forces.

In 2011 Yousef et al. reported Saudi Aramco's success in increasing the recoverable Original Oil in Place (OOIP) by 16-18% through low salinity waterflooding in composite rock samples from the Saudi Arabian carbonate reservoirs. According to Saudi Aramco, wettability alteration was the primary contributor to their experimental success. Research on wettability and imbibition uncovered various controlling parameters such as brine composition, pH, and temperature. In 1996, Milner proved in his Ph.D. thesis that although monovalent ions are too weak to prevent the crudes' adherence onto calcite, strong hydrated forces might exist for higher concentrations of divalent ions which promote sufficient short-range repulsive forces. Similarly, Zhang et al. (2006) discussed in the paper, submitted to the Journal of Energy and Fuel, titled "Wettability Alteration and Improved Oil Recovery in Chalk: The

Effect of Calcium in the Presence of Sulfate”, the catalytic role of the divalent ion  $\text{Ca}^{2+}$  in promoting imbibition and altering wettability.

Zahid et al. (2012) ran experimental investigations to define the potential for oil recovery increase through low salinity water flooding in both carbonate and outcrop chalk core plugs. The experiment was designed to initially flood the core plugs with seawater followed by sequential injection of various diluted seawater. Zahid et al. (2012) were conscious of the possible influence of capillary end effect, thus applied precautionary stepwise flowrate increase. Parameters of interest including oil recovery, ion-rock interaction, and wettability changes were studied at both surface and reservoir temperatures. Experimental results revealed that a substantial increase in oil recovery was possible through the diluted versions of seawater, but only in the carbonate core sample and under a high temperature ( $90^{\circ}\text{C}$ ). Zahid et al. (2012) concluded that as the salinity of the injected brine dropped, fines migration increased pressure drop across the core plug and blocked pore throats diverting the flow to non-swept zones which improved the microscopic efficiency. Additionally,  $\text{Ca}^{2+}$  production during diluted injection suggested rock dissolution as the contributing mechanism to the incremental recovery increase observed. Finally, a threshold injection rate was observed for each carbonate sample above which  $\text{Ca}^{2+}$  production seized.

Both Kyte et al. (1961) and Cuiec et al. (1994) experimental results have recorded an increase in oil recovery from strong/intermediate water-wet carbonates as the temperature increased. Additionally, Saner et al. (1991) studies yielded analogous conclusions that reported an increase in the water-wetness in a calcium carbonate core as the temperature grew higher. The 2006 work presented in PE/DOE Symposium on Improved Oil

Recovery by Tweheyo et al. evaluated the effect of varying ratios of  $\text{Ca}^{2+}$  and  $\text{SO}_4^{2-}$ , which literature cites as determining ions that greatly impact the surface charge of carbonate rocks, on wettability alteration and spontaneous imbibition under various temperatures. The experiment was conducted under temperature varying between 40-130°C on out-crop chalk samples aged for 4-6 weeks at 90°C in a modified crude with a 2 KOH-mg/g acid number. Tweheyo et al. (2006) concluded the following:

- High recovery was achieved under high temperatures and calcium-sulfate ratio given that the injection operates under the solubility limit of  $\text{CaSO}_4$ , a compound that the precipitation of which is controlled by magnesium concentration.
- Interfacial force that traps oil is minimized by both calcium and magnesium.
- The key determining ion that promotes wettability alteration from oil-wet to water-wet is sulfate.
- Calcium and magnesium encourage wettability transition by lowering the characteristic temperature requirement.

Majority of available literature addresses LSWF from a geochemical point of view. Recent studies stress the importance of fluid-fluid interactions, for brine-crude oil (micro-dispersion) interactions are dominant contributors of improved oil recovery in carbonate formations. According to Mahzari and Sohrabi (2015), micro-dispersion mechanism consists of micelles of water covered by surface active components in the oil phase. Tests performed on brines of varying salinity and different crudes by Alhammadi et al. (2017) showed that the micro-dispersion formation relates to oil recovery on one hand and the salinity range on the other, they concluded that there is a direct proportionality between micro-

dispersion amount and oil recovery. Aljaberi and Mehran (2019) utilized the results of waterflood experiments from a Middle Eastern carbonate reservoir to develop a new LSWF modelling approach, simulation results agreed with literature on the leading role of wettability alteration. Moreover, the research highlighted the importance of residual oil saturation reduction and shift in the relative permeability curves (for both oil and water) to achieve a successful history match. Prediction of the latter could be accomplished by studying the relationship between micro-dispersion and oil recovery. Expansion of this field of study is hindered however by the lack of a commercial simulator that can mimic this mechanism.

Singh and Sarma (2021) analyzed major LSWF field cases; conducting a comparative assessment of realized incremental recovery versus expected value generated from laboratory experiments and simulation runs. Singh and Sarma (2021) observed that the positive impact achieved from field application was not as high as the reported values from preparatory studies. The paper recommends laboratory test regimes that honor site specific reservoir conditions and use representative samples to yield relevant results. Singh and Sarma (2021) encourage thorough analysis of major factors such as formation and brine composition, rock wettability, oil-water interfacial tension, and geochemical reaction before initiation of field scale LSWF. Limitations and certainties could be detected and alleviated by designing a competent surveillance program and collecting field data at regular intervals.



# Chapter 2





## Chapter 2: Methods

### 2.1 Research Design

This section of the report shares the designed methodological procedure to achieve the set experimental objectives. Procedure can be divided into two stages, Figure 4 shares stage 1 and Figure 5 shares stage 2:

- Stage 1A: Core plug preparation and Petrophysical properties measurement.
- Stage 1B: Synthetical preparation of brine and seawater and Fluid properties measurement
- Stage 2A: Core sample selection, categorization, saturation, and aging.
- Stage 2B: IOR process (Low salinity slug flood) and post IOR analysis.

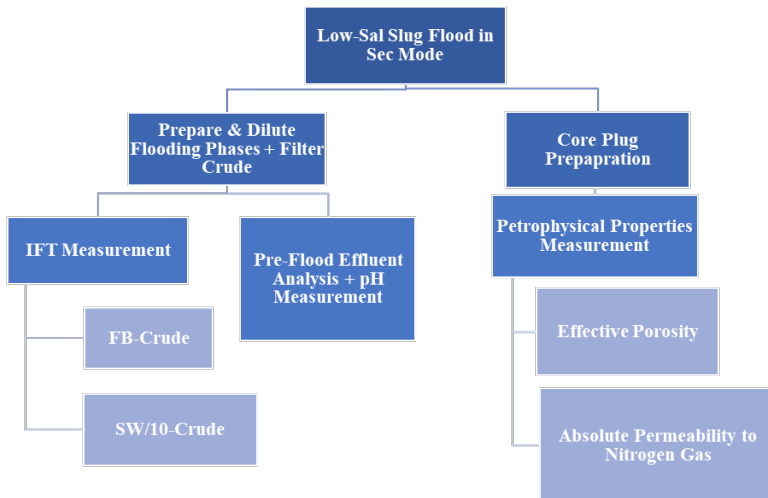


Figure 4: Stage 1 of Research Methodology

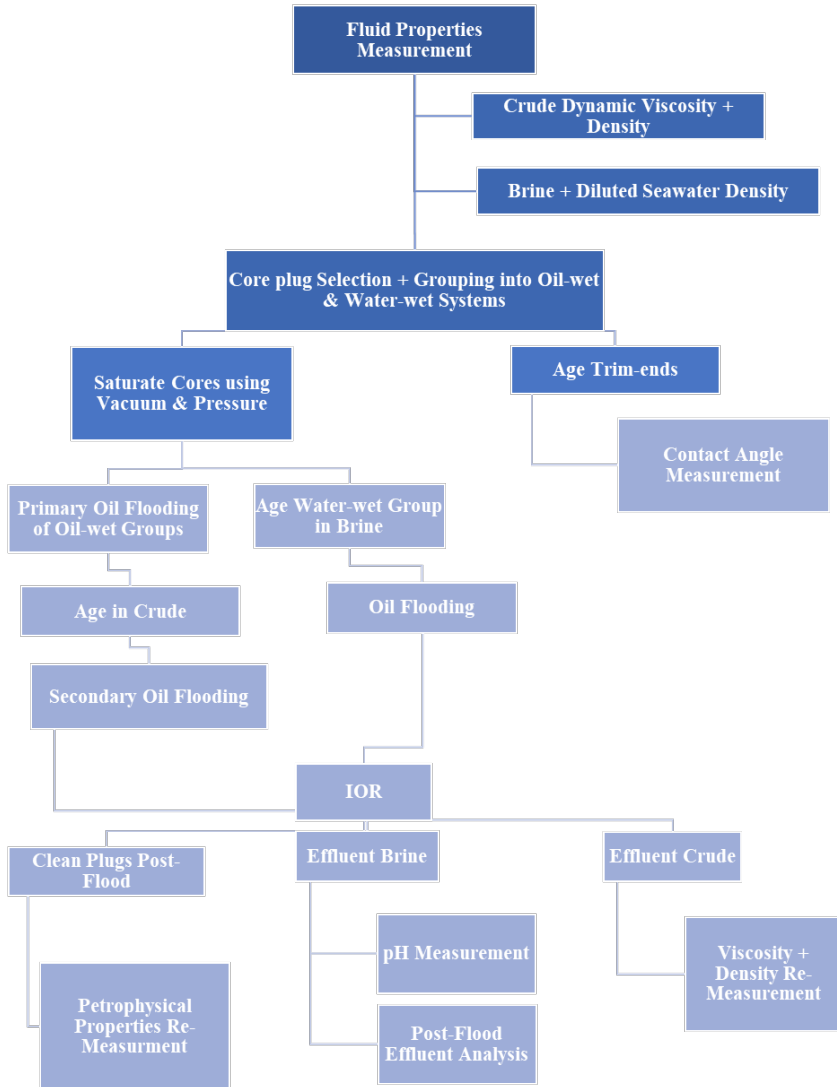


Figure 5: Stage 2 of Research Methodology

## 2.2 Data Collection

### 2.2.1 Core Samples and Petrophysical Properties

Forty horizontal core samples acquired from supplier (belonging to groups: ZE-1 and ZE-2) were cleaned, dried in a conventional drying oven, weighed, and their average dimensions measured using a vernier caliper. Consequently, effective porosity and absolute permeability to Nitrogen gas were measured to select 16 samples and group them into 4 categories according to lithology, permeability, and intended wettability.

Core samples were received from supplier saturated by only water-base mud, they were retrieved from a dry reservoir. As such, samples were sufficiently cleaned from salts using Soxhlet extractor (Figure 6), an apparatus typically used in routine core analysis.

Samples were placed in the Soxhlet thimble. The flask sitting on a heating mantle was part filled with solvent. In most routine core analysis, this will be toluene initially but, in this case, only methanol was used due to absence of hydrocarbons. When the solvent is sufficiently heated, it evaporated traveling up the side arm, bypassing the sample chamber, to the condenser. At which point, the solvent vapor condenses and falls into the Soxhlet thimble containing the plugs. As the hot solvent fills the chamber, it diffuses into the pores of the core and dissolves unwanted salts. The distilled solvent slowly fills the sample chamber, eventually submerging the core samples. When the level of solvent reaches the siphon point, the solvent and dissolved salts reflux from the thimble into the bottom flask. The cleaning process continued for 36 hours, then samples were tested by silver nitrate and found clean (no white precipitate).



Figure 6: Soxhlet Extractor

Effective porosity, which is the ratio of interconnected pore volume to bulk volume, was measured using the Poroperm device by Vinci Technologies (Figure 7). This apparatus uses Boyle-Mariotte's Law to provide grain volume, the governing relationship of which is derived as follows:

$$P_{ref}V_{ref} = P_{exp}V_{exp} \dots \dots \dots \text{Equation 1}$$

$$V_{exp} = V_{ref} + V_{matrix} - V_{grain} \dots \dots \dots \text{Equation 2}$$

$$V_{grain} = (V_{ref} + V_{matrix}) - \frac{P_{ref}V_{ref}}{P_{exp}} \dots \dots \dots \text{Equation 3}$$

$$V_{pore} = V_{bulk} - V_{grain} = \left(\frac{\pi LD^2}{4}\right)_{core} - V_{grain} \dots \dots \dots \text{Equation 4}$$

$P_{ref}$ : Reference Pressure (initial pressure), psi

$V_{ref}$ : Reference Volume (initial volume), cc

$P_{exp}$ : Expanded Pressure (final pressure), psi

$V_{exp}$ : Expanded Volume (final volume), cc

$V_{ref}$ : Reference Cell Volume, cc

$P_{ref}$ : Reference Cell Pressure, psi

$V_{matrix}$ : *Matrix Cup Volume, cc*

$(\frac{\pi LD^2}{4})_{core}$ : *Volume of Cylindrical Core Plug, cc*

The pore volume is easily computed using the presented equation above since both pressure at reference cell and matrix cup are recorded once stabilized, and volumes of reference cell and matrix cup are constants given by the Poroperm operator manual [ $V_{ref} = 64.258 \text{ cc}$ ,  $V_{matrix} = 101.214 \text{ cc}$ ]. Thus, solving this equation is simple mathematics. Results for limestone and dolomite samples are presented in Tables 1 and 2 porosity computed by device is that to Nitrogen gas, which is always greater than that to liquid (such as brine). The smaller volume of gases allows them to saturate smaller pore spaces governed by high capillary pressure at lower expanded pressure. Porosity to liquid can be calculated by the simple steps below:

1. Measure core dry weight.
2. Saturate core with brine.
3. Measure saturated weight. Find brine weight by subtracting dry weight from saturated weight.
4. Calculate brine volume by dividing brine weight by density.
5. Porosity to liquid is ratio of brine volume to bulk volume.

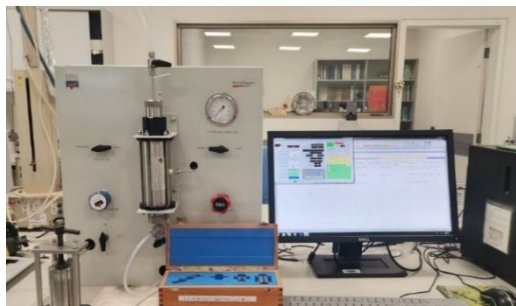


Figure 7: Poroperm

Permeability, ability to flow or transmit a particular fluid through a rock, was measured using the Poroperm device by Vinci Technologies as well. The calculation of absolute permeability to Nitrogen is derived from Darcy's law corrected for gas flow (Eq 5). Nitrogen is compressible, as it flows towards the downstream end of the core sample and pressure decreases, nitrogen gas expands and its velocity increases. Moreover, Nitrogen like all other gases has measurable velocity at pore walls. Thus, it does not meet the conditions of Darcy's law. The equivalent liquid permeability can be calculated using Klinkenberg correction factor (b) through Equation 6; Poroperm device automatically computes this value. Results of limestone and dolomite samples are presented in Tables 1 and 2.

$$k_g = \frac{2\mu Z T P_{atm} L Q_{atm}}{A T_{atm} (P_{upstream}^2 - P_{downstream}^2)} \dots \dots \dots \text{Equation 5}$$

$$k_l = \frac{k_g}{1 + \frac{b}{\left(\frac{P_{upstream} + P_{downstream}}{2}\right)}} \dots \dots \dots \text{Equation 6}$$

$k_g$ : permeability to gas, D

$\mu$ : gas viscosity, cp

$Z$ : mean gas compressibility factor

$T$ : mean temperature of flowing gas

$P_{atm}$ : atmospheric pressure, atm

$L$ : length of sample, cm

$Q_{atm}$ : atmospheric gas flow rate at  $P_{atm}$ ,  $\frac{cm}{s}$

$A$ : cross sectional area of culinder,  $cm^2$

Table 1: Limestone Group ZE-1 Average Dimensions and Petrophysical Properties

Sample Name	Dia (mm)	Length (mm)	Bulk Vol (cc) L*A	Weight (g)	Grain Vol. (cc)	Grain density (g/cc)	Pore Vol.(cc)	Porosity	Kg (mD)	Single point empirical KL (mD)	Darcy condition granted
1	38.31	50.67	58.41	126.77	47.02	2.696	11.39	0.195	33.733	28.172	OK
2	38.21	50.81	58.26	127.47	47.34	2.693	10.92	0.187	17.123	13.798	OK
3	38.3	50.78	58.5	126.83	46.96	2.701	11.54	0.197	19.148	15.518	OK
4	38.01	50.92	57.78	130.59	48.59	2.688	9.19	0.159	5.407	3.886	OK
5	38.27	50.78	58.41	131.7	49.1	2.682	9.31	0.159	17.949	14.118	OK
6	38.03	50.79	57.69	125.65	46.61	2.696	11.08	0.192	12.28	9.364	OK
7	37.83	50.85	57.15	121.46	45.1	2.693	12.05	0.211	13.69	10.544	OK
8	38.32	50.84	58.63	125.62	46.63	2.694	12	0.205	11.577	8.867	OK
9	38.02	50.68	57.54	130.65	48.74	2.681	8.8	0.153	13.838	10.655	OK
10	38.29	50.85	58.55	131.81	49.12	2.683	9.43	0.161	17.889	14.444	OK
11	37.86	50.88	57.28	126.46	46.85	2.699	10.43	0.182	8.263	6.114	OK
12	38.22	50.92	58.42	131	48.75	2.687	9.67	0.165	13.858	11.055	NO
13	38.01	50.89	57.75	130.1	48.5	2.683	9.25	0.16	18.969	14.999	OK
14	38.26	51	58.63	127.84	47.45	2.694	11.18	0.191	1.768	1.244	NO
15	38.07	50.88	57.92	130.25	48.5	2.686	9.42	0.163	7.374	5.482	OK
16	38.28	50.97	58.66	126.24	46.81	2.697	11.85	0.202	8.999	6.739	OK
17	38.26	50.9	58.52	128.83	48.09	2.679	10.43	0.178	230.612	210.804	OK
18	37.92	50.98	57.57	127.38	47.48	2.683	10.09	0.175	18.342	14.462	OK
19	38.23	50.81	58.32	131.21	48.97	2.68	9.35	0.16	38.799	32.479	OK
20	37.85	50.8	57.16	122.11	45.44	2.687	11.72	0.205	139.879	125.223	OK

Table 2: Dolomite Group ZE-2 Average Dimensions and Petrophysical Properties

Sample Name	Dia (mm)	Length (mm)	Bulk Vol (cc) L*A	Weight (g)	Grain Vol. (cc)	Grain density (g/cc)	Pore Vol.	Porosity	Kg (mD)	Single point empirical KL (mD)	Darcy condition granted
1	38.09	50.98	58.09	138.32	48.82	2.833	9.268	0.16	15.164	11.777	OK
2	37.67	50.83	56.65	143.48	50.42	2.846	6.235	0.11	7.558	5.424	OK
3	37.83	50.85	57.15	145.98	51.34	2.843	5.809	0.102	4.077	2.724	OK
4	38.13	50.78	57.99	138.62	49.27	2.813	8.72	0.15	186.76	168.707	OK
5	37.64	50.88	56.62	141.66	50.44	2.808	6.179	0.109	0.087	0.051	NO
6	37.76	50.76	56.84	139.3	49.5	2.814	7.345	0.129	12.224	9.325	OK
7	37.74	50.95	57	135.93	48.04	2.83	8.963	0.157	256.874	235.588	OK
8	37.7	50.92	56.84	142.9	51.26	2.788	5.576	0.098	1.925	1.361	OK
9	38.12	50.88	58.07	146.29	51.58	2.836	6.488	0.112	28.266	23.217	OK
10	37.92	51.18	57.8	138	48.98	2.818	8.822	0.153	130.657	116.656	OK
11	38.18	50.75	58.1	137.4	48.79	2.816	9.308	0.16	114.176	101.142	OK
12	37.8	50.97	57.2	142.38	51.02	2.791	6.185	0.108	4.624	3.142	OK
13	38.14	50.77	58	144.56	50.96	2.837	7.042	0.121	35.217	29.344	OK
14	38.1	51.01	58.16	141.15	50.08	2.819	8.081	0.139	91.039	79.812	OK
15	37.68	50.95	56.81	129.93	46.2	2.812	10.611	0.187	689.004	649.514	OK
16	37.63	50.78	56.47	142.77	50.84	2.808	5.626	0.1	1.633	1.144	OK
17	37.78	50.84	56.99	138.62	49.22	2.817	7.774	0.136	20.149	16.227	OK
18	37.65	50.89	56.66	138.76	49.43	2.807	7.234	0.128	9.743	7.301	OK
19	37.74	50.82	56.85	130.38	46.35	2.813	10.5	0.185	--	--	--
20	37.63	50.91	56.62	124.05	43.97	2.821	12.65	0.223	329.169	304.145	OK



### 2.2.2 Fluids

Crude taken from Asab onshore oil field in UAE, operated by Abu Dhabi Company for Onshore Petroleum Operation Ltd (ADCO), of specific gravity 0.8338 was filtered through an 8.0 micro-meter filter paper multiple times prior to any laboratory application. Investigation revealed no asphaltene precipitation. Crude dynamic viscosity value of 7.1045 cp was measured using rolling ball viscometer at ambient temperature (20°C). The oil is sweet and has no H<sub>2</sub>S gas.

Asab brine of Total Dissolved Salts (TDS) 143,008 ppm was synthetically prepared in the laboratory (using set up depicted by Figure 9) according to specifications listed in Tables 3 and 4. Salts were added in the following order: least soluble salts first followed by those required at smaller amounts. Sodium chloride is added last due to its high solubility and concentration. Otherwise, water will be sufficiently saturated by NaCl and will no longer accept Chloride from salts of lower solubility such as CaCl<sub>2</sub>. Density of prepared brine was found to be 1.101g/cc simply by using a pycnometer of 50cc volume and lab weighing balance (Figure 8). This brine will be used as the high salinity water in the experiment. Both Asab crude and brine were obtained from well SB-0567.

Table 3: Asab Brine Ion Content

Cations Analyzed (mg/L)		Anions Analyzed (mg/L)	
Na <sup>+</sup>	44,261	Cl <sup>-</sup>	96,566
Ca <sup>++</sup>	13,840	SO <sub>4</sub> <sup>-</sup>	885
Mg <sup>++</sup>	1,604	HCO <sub>3</sub> <sup>-</sup>	332

Table 4: Composition of Asab Brine

Chemicals	1 Litre (g)
NaHCO <sub>3</sub> (Anhy)	0.46
Na <sub>2</sub> SO <sub>4</sub> (Anhy)	1.31
NaCl	111.12
CaCl <sub>2</sub> (Anhydrous)	38.32
MgCl <sub>2</sub> .6H <sub>2</sub> O	13.42
TDS (ppm)	143,008

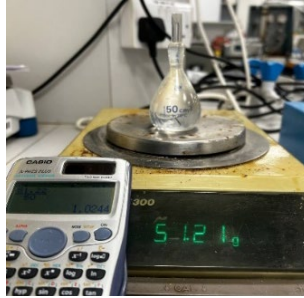


Figure 8: Pycnometer and Weighing Balance

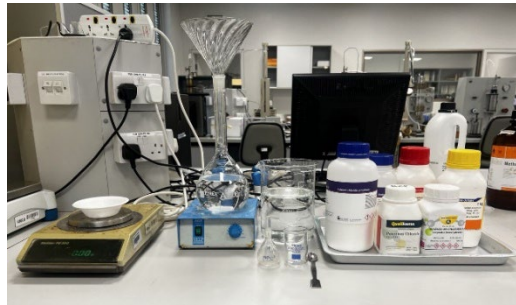


Figure 9: Brine Preparation Setup

Seawater of Total Dissolved Solids (TDS) 53,936 ppm was synthetically prepared in the laboratory according to specifications listed in Tables 5 and 6. Density of prepared water was found to be 1.0244 g/cc.

Table 5: Seawater Ion Content

Cations Analyzed (mg/L)		Anions Analyzed (mg/L)	
Na+	16,767	Cl -	30,924
Ca++	690	SO4 -	3,944
Mg++	2,132	HCO3 -	123
K+	672		

Table 6: Composition of Seawater

Chemicals	1 Litre (g)
NaHCO3 (Anhy)	0.17
Na2SO4 (Anhy)	5.83
NaCl	37.71
CaCl2 (Anhydrous)	1.91
KCl	1.28
MgCl2.6H2O	17.83
TDS (ppm)	53,936

Low salinity water required for the IOR experiment was prepared by diluting the seawater by a factor of 10. Using the simple mathematical relationship below, the volume required to prepare 1 liter of SW/10 was found to be 100 cc of seawater diluted by 900 cc of distilled water. Density of low salinity seawater is 0.9954 g/cc.

$$C_1V_1 = C_2V_2 \dots \dots \dots \text{Equation 7}$$

$$C_1 = 53,936 \text{ ppm}$$

$$C_2 = \frac{C_1}{10} = 5,393.6 \text{ ppm}$$

$$V_2 = 1000 \text{ cc}$$

$$V_1 = \frac{C_2V_2}{C_1} = \frac{5,393.6 \times 1000}{53,936} = 100 \text{ cc}$$

Diluted seawater was selected as the low salinity water because the amount of water required to dilute seawater (50,000 ppm) to a lower salinity of 5,000 ppm is much less than that required to dilute Asab brine (143,008 ppm).

### 2.2.3 System Selection and Core Saturation

- Samples were categorized based on lithology and subcategorized into groups, in which members have similar permeability (Tables 7 and 8).
- 12 samples were made oil-wet through primary oil flooding followed by aging in Asab crude.
- 4 samples were made water-wet through aging in Asab brine.

Table 7: Core Samples Classification for Limestone Group ZE-1 According to the Intended Investigation

Sample Number	Group ID	Introduced Wettability	Permeability Classification	Permeability md	Mineralogy
2	ZE-1	oil-wet	High	13.798	Limestone
5	ZE-1	oil-wet	High	14.118	Limestone
6	ZE-1	water-wet	High	9.364	Limestone
7	ZE-1	water-wet	High	10.544	Limestone
8	ZE-1	water-wet	High	8.867	Limestone
9	ZE-1	water-wet	High	10.655	Limestone
10	ZE-1	oil-wet	High	14.444	Limestone
18	ZE-1	oil-wet	High	14.462	Limestone

Table 8: Core Samples Classification for Dolomite Group ZE-2 According to the Intended Investigation

Sample Number	Group ID	Introduced Wettability	Permeability Classification	Permeability md	Mineralogy
1	ZE-2	oil-wet	High	11.777	Dolomite
3	ZE-2	oil-wet	Low	2.724	Dolomite
6	ZE-2	oil-wet	High	9.325	Dolomite
8	ZE-2	oil-wet	Low	1.361	Dolomite
12	ZE-2	oil-wet	Low	3.142	Dolomite
16	ZE-2	oil-wet	Low	1.144	Dolomite
17	ZE-2	oil-wet	High	16.227	Dolomite
18	ZE-2	oil-wet	High	7.301	Dolomite

Selected samples were saturated using vacuum and pressure method. Initially vacuum was applied to remove all air in core holder and sample pores. Once negative pressure was recorded, vent was opened to equalize the pressure between the core holder and brine flask, saturating all large pores in the process. Finally, pressure was applied to force brine into smaller pores and fully saturate the sample. This procedure is both simple and effective. A pressure of approximately 1800 psi was required to force brine into core pores, which is 18 times higher than that applied to saturate cores with nitrogen during petrophysical properties measurement.

## 2.2.4 Oil Flooding

### 2.2.4.1 Primary Oil Flooding

Cores in Tables 7 and 8 saturated with Asab brine and intended to be oil wet underwent primary oil flooding by Asab crude. Injectivity issues and possible permeability impairment were encountered due to introducing crude to dry well samples (Figure 11). Another possibility would be incompatibility between crude and brine; thus, a separability test was conducted to investigate emulsion formation as possible cause for deposition hindering flow. Figure 10 shows a comparative study conducted between Asab crude-Asab brine system (Righthand side tube) and Bu Hasa crude-Asab brine system (Lefthand side tube), both systems displayed

similar behavior in which no emulsion was formed and crude-brine segregation occurred gradually due to gravity effect.

Faramarzi-Palangar et al. (2021) suggested the following to alleviate injectivity issues and possible permeability impairment in carbonates during laboratory experiments: replace dead reservoir oil with synthetic oil (n-Decane). Decalin should be used as a buffer fluid between synthetic oil and reservoir oil to prevent asphaltene precipitation. Such a solution is not applicable in this study because we are interested in the IFT between Asab crude and displacing fluids.

The following conclusion was made after concluding primary oil flooding, both limestone and dolomite samples are initially highly water wet with strong capillary forces trapping water droplets and hindering introduction of crude to the pores. This was verified by the high oil cut and very early oil breakthrough. Results of primary oil flooding can be found in Tables 9 and 10.



Figure 10: Separability Test



Figure 11: Precipitate at Limestone Core-Head

Table 9: Oil-Wet Limestone Primary Oil Flood Results (ZE1)

Sample ID	Dry wt. (gm)	Sat. wt. (gm)	Press. (psi)	Time (sec)	Volume (cc)	Water produced (cc)	Pore vol. (cc)	Swi (%)
2	127.47	134.77	50	60	0.5	2.95	6.63	55.5
5	131.7	139.04	480	60	0.04	3.1	6.67	53.5
10	131.81	138.9	480	60	0.04	3.95	6.44	38.7
18	127.38	136.54	480	60	0.04	3.75	8.32	54.9

Table 10: Oil-Wet Dolomite Primary Oil Flood Results (ZE2)

Sample ID	Dry wt. (gm)	Sat. wt. (gm)	Press. (psi)	Time (sec)	Volume (cc)	Water produced (cc)	Pore vol. (cc)	Swi (%)
1	138.32	144.61	450	60	0.02	3.95	5.71	30.8
6	139.3	144.54	450	60	0.01	2.6	4.76	45.4
17	138.61	143.96	500	60	0.33	2.3	4.86	52.7
18	138.75	143.25	500	60	0.02	2	4.09	51.1
3	145.98	149.98	500	60	0.03	2.2	3.63	39.4
8	142.9	147.03	500	60	0.04	2.6	3.75	84
12	142.38	147.93	500	60	0.03	2.2	5.04	56.3
16	142.77	148	500	60	0.04	2.5	4.75	47.4

#### 2.2.4.2 Aging

An oil wettability was introduced to the samples by aging them in Asab crude for 4 weeks (Figure 13). Whereas the samples intended to be water wet were aged in Asab brine for a similar period (Figure 12).



Figure 12: Samples Aged in Brine

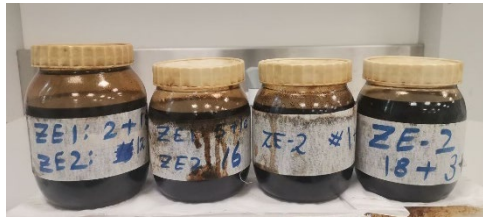


Figure 13: Samples Aged in Crude

#### 2.2.4.3 Secondary Oil Flooding

Samples aged in Asab crude underwent secondary oil flooding after 4 weeks to investigate success of wettability alteration. This was achieved using the same flooding apparatus utilized during primary flooding (Figure 14). This device has the following limitation, overburden pressure must be greater than the injection pressure by at least 400 psi, which is the zero-confining stress of the core sleeve. Otherwise, oil introduced by injection will not be confined to enter through core head but would also seep to the sides of the cylindrical core plug, as such lab conditions would fail to imitate field practice and results will no longer be representative.



Secondary oil flooding of both limestone and dolomite cores confirmed the success of aging in altering the wettability, water was produced beyond the initially recorded irreducible water saturation. All samples were flooded for the same period of time (24 hours) but the size of the flood differed, a smaller flood size is indicative of tighter flow paths that will be less efficient in delivering the crude during IOR. Secondary oil flooding results can be found in Tables 11 and 12.



Figure 14: Core Flooding Apparatus

Table 11: Oil-Wet Limestone Secondary Oil Flood Results (ZE1)

Sample ID	Pore vol. (cc)	Flood size (* PV)	Press. (psi)	Time (sec)	Volume (cc)	Water produced (cc)	Swi (%)
2	6.63	9.5	750	60	0.202	0.7	44.9
5	6.67	2.7	750	60	0.019	0.25	49.8
10	6.44	5.0	750	60	0.066	0.15	36.3
18	8.32	2.0	750	60	0.048	0.12	53.5

Table 12: Oil-Wet Dolomite Secondary Oil Flood Results (ZE2)

Sample ID	Pore vol. (cc)	Flood size (* PV)	Press. (psi)	Time (sec)	Volume (cc)	Water produced (cc)	Swi (%)
1	5.71	3.5	750	60	0.056	0.15	28.2
6	4.76	1.05	750	60	0.069	0.23	40.5
17	4.86	2.7	750	60	0.067	0.15	49.6
18	4.09	3.2	750	60	0.075	0.09	48.9
3	3.63	3.1	750	60	0.059	0.12	36.1
8	3.75	2.9	750	60	0.055	0.05	82.7
12	5.04	6.5	750	60	0.035	0.15	53.4
16	4.75	1.3	750	60	0.075	0.2	43.1

#### 2.2.4.4 Water-Wet Samples Oil Flooding

Samples designated to be water wet were removed from brine, in which they were aged, and flooded with Asab crude. This process imitates primary drainage in field conditions, i.e., migration of hydrocarbons from source rock to initially water wet reservoir rock. During oil flooding, water saturation decreases, and oil saturation increases until irreducible water saturation is reached (100% oil cut). At the conclusion of the process, introduced crude within sample, which translates to OOIP, was found by measuring amount of brine produced. Results of this process can be found in Table 13.

Table 13: Water-Wet Limestone Samples Oil Flood Results (ZE1)

Sample ID	Dry wt. (gm)	Sat. wt. (gm)	Press. (psi)	Time (sec)	Volume (cc)	Water produced (cc)	Pore vol. (cc)	Swi (%)
6	125.65	136.91	750	60	0.067	4	10.22	60.9
7	121.46	132.72	430	60	0.6	5.6	10.22	45.2
8	125.62	137.40	430	60	0.6	5.6	10.7	47.7
9	130.65	139.23	750	60	0.077	5.6	7.79	48.7

### *2.2.5 Improved Oil Recovery*

Improved oil recovery process of all samples at irreducible water saturation was conducted by introducing a certain slug size of low salinity seawater then continuously flooding the core with high salinity brine until 100% water cut was realized. Slug size 0.1, 0.2, 0.3, and 0.4 were explored in this thesis to define the optimum slug size. IOR results can be found in Tables 14 -17 and Figures 15-18.

Table 14: IOR Results of Water-Wet High-k Limestone Samples

Sample #	OOIP	Eff. Pore Volume	Low-Salinity Slug Flood			High-Salinity Continuous Flood			Cum. Recovery		Sor
			Slug Size	Oil Produced	Slug Recovery	Oil Produced	(Np/N) *100	%PV	(Np/N) *100	%PV	
	cc	cc	%PV	cc	(Np/N) *100	%PV	cc	(Np/N) *100	%PV	(Rem. Oil/PV) *100	
9	4	7.79	10	0.83	20.75	10.65	0.2	25.75	13.22	38.13	
6	4	10.22	20	1.1	27.5	10.76	0.5	40	15.66	23.48	
7	5.6	10.22	30	1.78	31.79	17.42	1.45	57.68	31.6	23.19	
8	5.6	10.7	40	2.2	39.29	20.56	1.1	58.93	30.84	21.5	

Table 15: IOR Results of Oil-Wet High-k Limestone Samples

Sample #	OOIP	Eff. Pore Volume	Low-Salinity Slug Flood			High-Salinity Continuous Flood		Cum. Recovery		Sor
			Slug Size	Oil Produced	Slug Recovery	Oil Produced	(Np/N) * 100	%PV		
	cc	cc	%PV	cc	(Np/N) * 100	%PV	cc	(Np/N) * 100	%PV	(Rem. Oil/PV) * 100
2	3.65	6.63	10	0.6	16.44	9.05	2.65	89.04	49.02	6.03
5	3.35	6.67	20	0.9	26.87	13.49	1.7	77.61	38.98	11.24
10	4.1	6.44	30	1.3	31.71	20.19	1.95	79.27	50.47	13.2
18	3.87	8.32	40	1.6	41.34	19.23	1.22	72.87	33.89	12.62

Table 16: IOR Results of Oil-Wet High-k Dolomite Samples

Sample #	OOIP cc	Eff. Pore Volume cc	Low-Salinity Slug Flood				High-Salinity Continuous Flood		Cum. Recovery		Sor
			Slug Size %PV	Oil Produced cc	Slug Recovery (Np/N) *100	%PV	Oil Produced cc	(Np/N) *100	%PV	(Rem. Oil/PV) *100	
1	4.1	5.71	10	0.25	6.1	4.38	0.55	19.51	14.01	57.79	
6	2.83	4.76	20	0.36	12.72	7.56	0.05	14.49	8.61	50.84	
17	2.45	4.86	30	0.2	8.16	4.12	0.3	20.41	10.29	40.12	
18	2.09	4.09	40	0.45	21.53	11	0.1	26.32	13.45	37.65	

Table 17: IOR Results of Oil-Wet Low-k Dolomite Samples

Sample #	OOIP	Eff. Pore Volume	Low-Salinity Slug Flood				High-Salinity Continuous Flood		Cum. Recovery		Sor
			Slug Recovery		Oil Produced		Oil Produced	Slug Recovery	(Np/N)*100	%PV	
			Slug Size	Oil Produced	Oil Produced	Slug Recovery					
	cc	cc	%PV	cc	(Np/N)*100	%PV	cc	(Np/N)*100	%PV	(Rem. Oil/PV)*100	
3	2.32	3.63	10	0.2	8.62	5.51	0.1	12.93	8.26	55.65	
8	2.65	3.75	20	0.85	32.08	22.67	0.05	33.96	24	46.67	
12	2.35	5.04	30	0.53	22.55	10.52	0.05	24.68	11.51	35.12	
16	2.7	4.75	40	1	37.04	21.05	0.05	38.89	22.11	34.74	

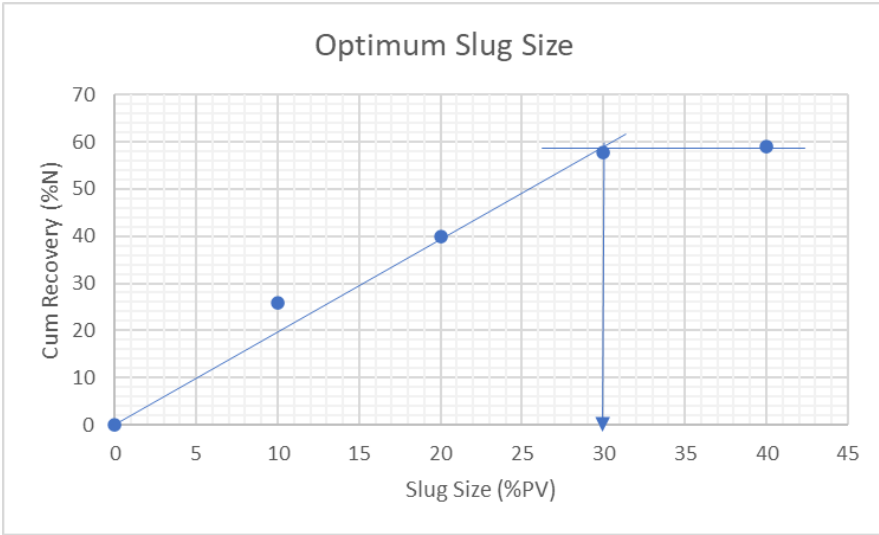


Figure 16: Optimum Slug-Size of Water-Wet High-k Limestone Group

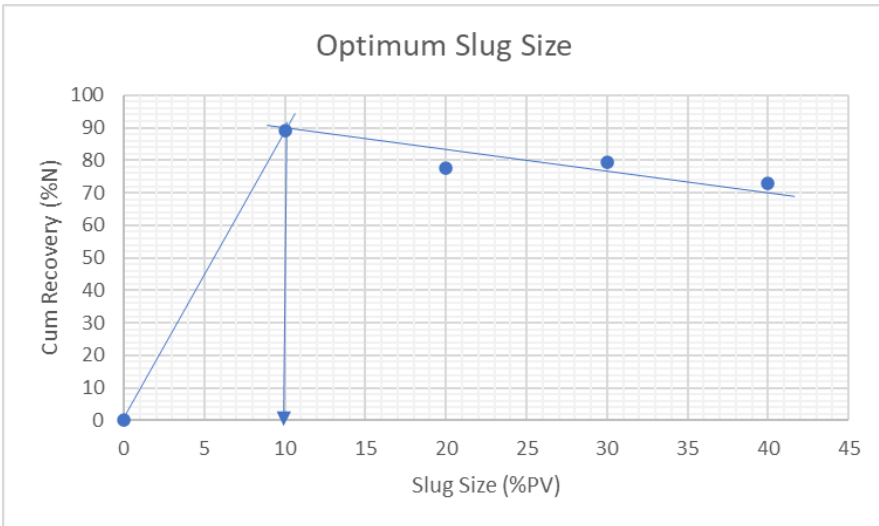


Figure 15: Optimum Slug-Size of Oil-Wet High-k Limestone Group



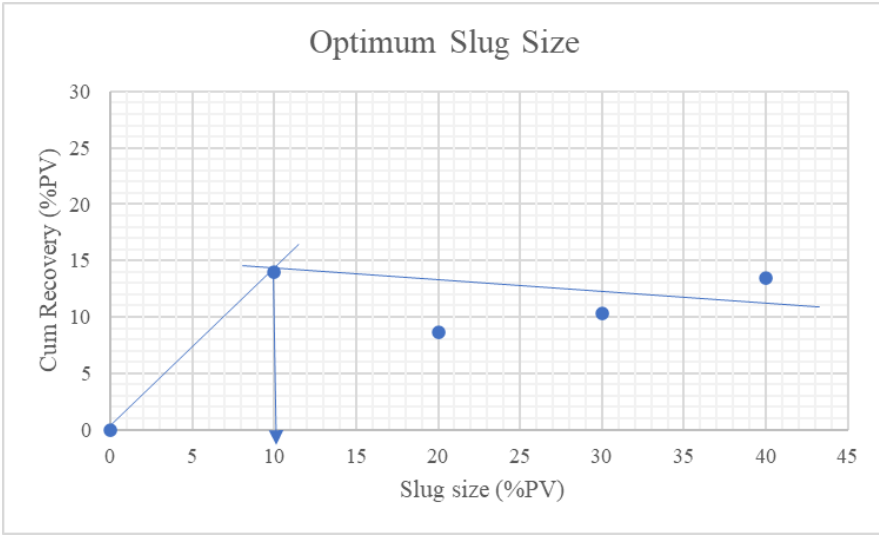


Figure 18: Optimum Slug-Size of Oil-Wet High-k Dolomite Group

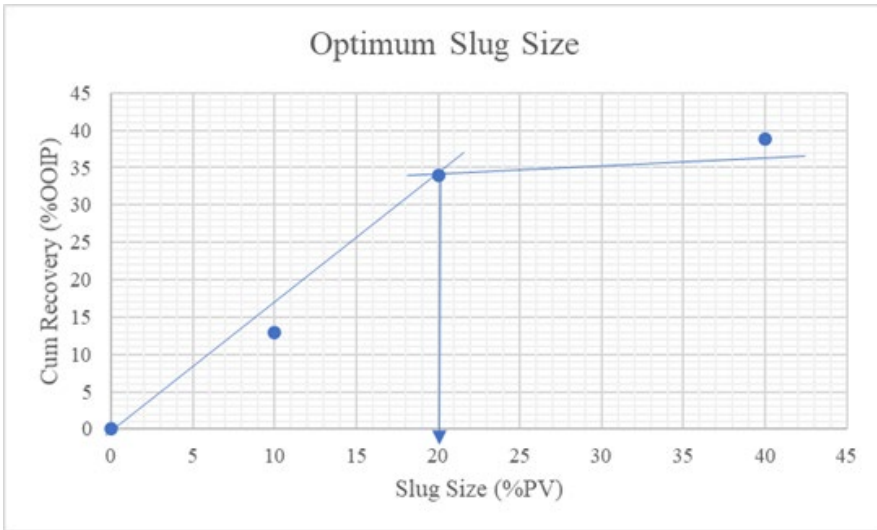


Figure 17: Optimum Slug-Size of Oil-Wet Low-k Dolomite Group

### 2.2.6 Interfacial Tension (IFT) Measurement

An interface of few molecular diameter in thickness separates the two immiscible phases (oil-water) present in the core during IOR. Interfacial tension results from the imbalance of forces at the interface which is due to the inward attraction of molecules on all sides and lack of outward attraction, this causes the surface to contract to the smallest possible area (Tiab & Donaldson, 2015). IFT has dimensions of force per unit length. Accurate measurement of the interfacial tension is essential and can lead to valuable insights into the phenomena taking place at the interface. Interfacial tension measurement of oil/formation brine and oil/low-salinity seawater was carried out using KRUSS Spinning Drop Tensiometer (Figure 19) at ambient temperature and pressure conditions. This test was conducted to investigate whether use of low-salinity water reduces IFT between displacing phase and oil; IFT is key factor that capillary force is directly proportional to. Reducing capillary force will increase capillary number which will help us achieve a higher displacement efficiency. Results are recorded in Tables 18-21 and Figures 20-23.



Figure 19: KRUSS Spinning Drop Tensiometer

Table 18: Summary of IFT Results for Asab Brine/Asab Crude System

Name	Value	Unit	Description
$\sigma$	9.786457 $\pm$ 0.075807	mN/m	Mean IFT and standard deviation
f rot	1499.5 $\pm$ 0.3	rpm	Mean rotational speed and standard deviation
T	22.8 $\pm$ 0.1	$^{\circ}$ C	Mean sample temperature
T Heating	23.0 $\pm$ 0.0	$^{\circ}$ C	Mean heating temperature and standard deviation
V	13.899 $\pm$ 0.053	$\mu$ L	Mean drop volume and standard deviation

Table 19: IFT Results for Asab Brine/Asab Crude System

Step Number	IFT (mN/m)	T ( $^{\circ}$ C)	Analysis Method	Drop Volume ( $\mu$ L)	Rotational Speed (rpm)
1	9.728033	22.9	Young-Laplace	13.936	1499.7
2	9.667881	22.8	Young-Laplace	13.859	1500
3	9.814089	22.9	Young-Laplace	13.959	1499.6
4	9.872721	22.9	Young-Laplace	13.947	1499.6
5	9.777937	22.8	Young-Laplace	13.892	1499.6
6	9.770534	22.8	Young-Laplace	13.838	1499.4
7	9.758156	22.8	Young-Laplace	13.826	1499
8	9.902306	22.7	Young-Laplace	13.939	1499.4

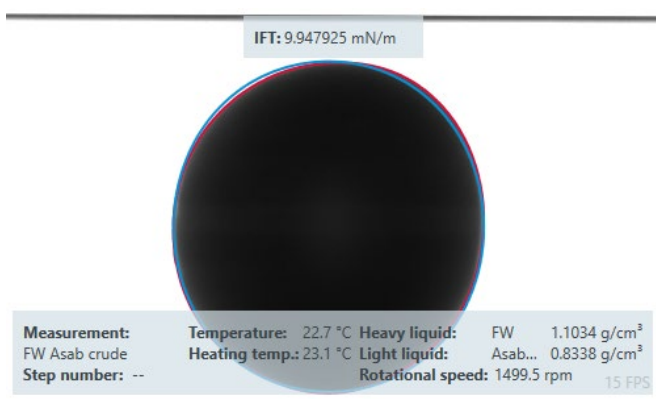


Figure 20: Oil Drop in Asab Brine

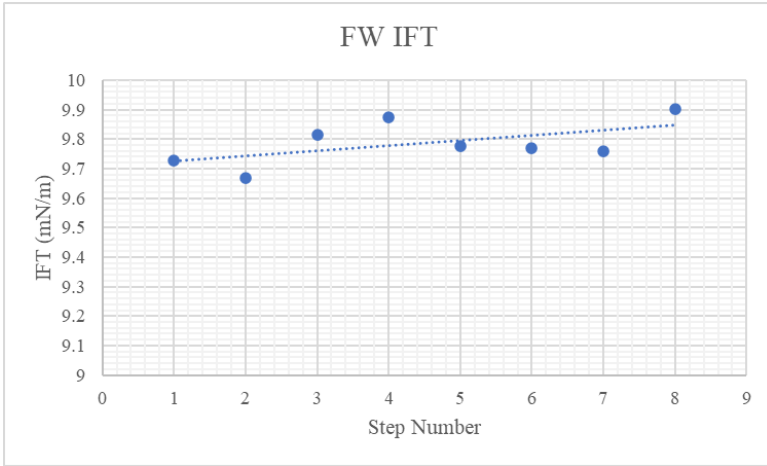


Figure 21: IFT Ascending Trend in Asab Brine

Table 20: Summary of IFT Results for Low-Salinity SW/Asab Crude System

Name	Value	Unit	Description
$\sigma$	4.099450 $\pm 0.160166$	mN/ m	Mean IFT and standard deviation
f rot	1499.6 $\pm 0.3$	rpm	Mean rotational speed and standard deviation
T	23.2 $\pm 0.4$	$^{\circ}\text{C}$	Mean sample temperature
T Heating	23.0 $\pm 0.0$	$^{\circ}\text{C}$	Mean heating temperature and standard deviation
V	11.656 $\pm 0.082$	$\mu\text{L}$	Mean drop volume and standard deviation

Table 21: IFT Results for Low-Salinity SW/Asab Crude System

Step Number	IFT (mN/m)	T (°C)	Analysis Method	Drop Volume (μL)	Rotational Speed (rpm)
1	4.436615	23.8	Young-Laplace	11.518	1499.5
2	4.404494	23.7	Young-Laplace	11.512	1499.7
3	4.371423	23.7	Young-Laplace	11.544	1500
4	4.295228	23.6	Young-Laplace	11.542	1499.8
5	4.285299	23.6	Young-Laplace	11.553	1500
6	4.272941	23.6	Young-Laplace	11.564	1499.7
7	4.261354	23.5	Young-Laplace	11.575	1499.6
8	4.210093	23.5	Young-Laplace	11.59	1499.6
9	4.185621	23.4	Young-Laplace	11.611	1499
10	4.148435	23.4	Young-Laplace	11.616	1499.3
11	4.137652	23.3	Young-Laplace	11.626	1499.6
12	4.091111	23.3	Young-Laplace	11.64	1499.8
13	4.077223	23.2	Young-Laplace	11.651	1499
14	4.043145	23.1	Young-Laplace	11.655	1499.6
15	4.025124	23.1	Young-Laplace	11.677	1499.7
16	4.014159	23	Young-Laplace	11.688	1499.4
17	4.008687	23	Young-Laplace	11.7	1500
18	4.005606	23	Young-Laplace	11.7	1499.5
19	3.988952	22.9	Young-Laplace	11.722	1499.7
20	3.985434	22.9	Young-Laplace	11.722	1499
21	3.962298	22.9	Young-Laplace	11.715	1499.7
22	3.97103	22.8	Young-Laplace	11.743	1499.7
23	3.945486	22.8	Young-Laplace	11.737	1499.7
24	3.936971	22.8	Young-Laplace	11.748	1499.8
25	3.938823	22.7	Young-Laplace	11.749	1500
26	3.927937	22.7	Young-Laplace	11.759	1499.6
27	3.935415	22.7	Young-Laplace	11.748	1499.6
28	3.918054	22.6	Young-Laplace	11.769	1499.5

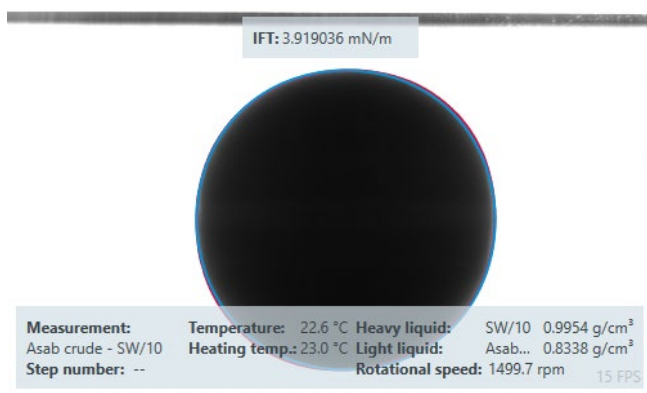


Figure 22: Oil Drop in Low-Salinity SW

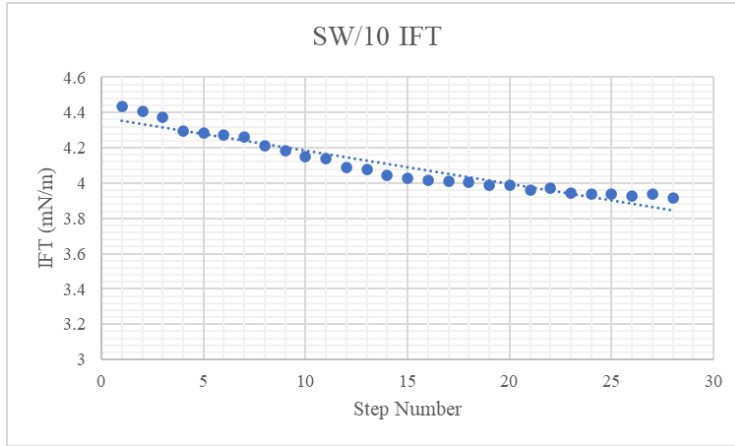


Figure 23: IFT Descending Trend in Low-Salinity SW

### 2.2.7 Contact Angle Measurement

Trim-ends from sample ZE1-3 were taken as representatives of the high permeability limestone group whereas those acquired from samples ZE2-9 and ZE2-2 represented dolomite high permeability and low permeability groups respectively using core trimmer (Figure 24). Consequently, trim-ends were cleaned from dust, weighed, and aged in crude and brine to represent the four groups on which IOR experiment was performed.

- Group 1: Limestone, high permeability, aged in brine to introduce water wetness.
- Group 2: Limestone, high permeability, aged in crude to introduce oil wetness.
- Group 3: Dolomite, high permeability, aged in crude to introduce oil wetness.
- Group 4: Dolomite, low permeability, aged in crude to introduce oil wetness.

Contact angle, a method used to quantify wettability of grain surface, was measured at ambient conditions for both limestone and dolomite trim ends. Wettability is defined by Anderson (1986) as the rock's preference to be in contact with one fluid rather than another, making it one of the key parameters that define fluid flow in porous media. Grain preference to fluid depends on various factors including crude heavy components, pore structure, aging time, rock mineral composition, and temperature (Graue et al., 2002; Salathiel, 1973).

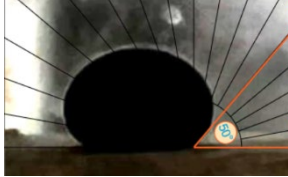

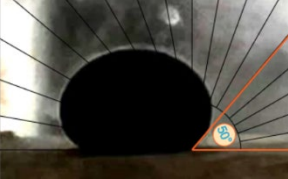
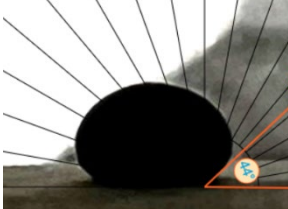
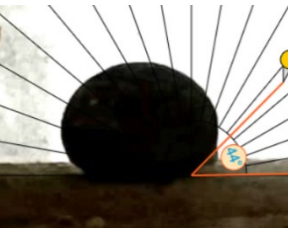
After three weeks of aging, trim ends were placed in low salinity seawater for 24 hours then formation brine for 72 hours in an effort to imitate flood conditions. Contact angles of emerging oil droplets are displayed in Table 22; conclusions were made according to Anderson's (1986) classification of wettability in terms of contact angle:

- Water-wet:  $0^{\circ}$ - $75^{\circ}$ .
- Intermediate-wet:  $75^{\circ}$ - $115^{\circ}$ .
- Oil-wet:  $115^{\circ}$ - $180^{\circ}$ .



Figure 24: Core Trimmer

Table 22: Measurement of Trim-Ends Contact Angle

Trim-End ID	Group	Before Aging (Initial Wettability)	After Aging + IOR (Final Wettability)
ZE1-3	1		
ZE1-3	2		No oil droplet observed
ZE2-9	3		No oil droplet observed
ZE2-2	4		No oil droplet observed



### *2.2.8 Effluent Analysis*

Carbonates exhibit reduced oil recovery when compared to sandstones, this is because such formations are preferentially oil wet, suffer negative capillary pressure, and are naturally fractured. Preferential oil wettability is promoted by the adsorption of negatively charged carboxylic component, present in the heavy end fractions of crude oil, onto positively charged carbonate surfaces. Negative capillary pressure in oil wet rock makes spontaneous imbibition in carbonates impossible. Natural fractures result in early water break through; injected water travels through the high permeability fractures instead of efficiently sweeping the matrix (Al-Hadhrami & Blunt, 2000). This makes improved oil recovery techniques essential for carbonate reservoirs to yield high recovery factors.

IOR methods, such as the topic of interest in this research, are capable of wettability improvement. Wettability, as discussed previously, is the relative adhesion of two fluids to a rock surface and ranges from strongly water-wet to strongly oil-wet. Effluent analysis post flood was conducted because ions in the displacing fluid play a crucial role in wettability alteration. Table 23 records the ionic concentration of the post flood effluent, comparisons with the ionic concentration pre-flood recorded in Table 3 helped in drawing conclusions of the mechanisms contributing to improved recovery. ICP was utilized to run the effluent analysis, limitation of device mandated dilution of formation water by 1000 to run test.

Table 23: Effluent Analysis of Cations Concentration

Group	ID	Mineralogy	Pre-Flood Wettability	k	Pre-Flood Cation Concentration			Post-Flood Cation Concentration		
					Ca	Mg	Na	Ca	Mg	Na
1	ZE1-8	limestone	water-wet	high	13840	1604	44261	18600	2155	57247
2	ZE1-2	limestone	oil-wet	high	13840	1604	44261	12340	1485	38410
3	ZE2-18	dolomite	oil-wet	high	13840	1604	44261	14720	1756	47282
4	ZE2-3	dolomite	oil-wet	low	13840	1604	44261	13720	1669	43260

# Chapter 3



## Chapter 3: Results and Discussions

### 3.1 Overview of the Main Findings

Despite the high permeability of samples ZE1 2,5,10,18 and ZE2 1,6,17,18, pressure drop required to achieve a relatively low flow rate is high, as recorded by column 4 of Tables 11 and 12. This could be due to high capillary force trapping fluids; this parameter is a function of IFT, contact angle, and pore radius.

Secondary oil flooding results recorded in Tables 11 and 12 prove success of aging in altering initial rock wettability to a more oil wet state. Comparing recorded Swir in Tables 9 and 10 with values in Tables 11 and 12, shows a decrease in the value; we were able to produce water beyond the initial 100% oil cut.

The optimum slug size of the four different experimental groups is as follows:

- Group 1: 30% PV (Figure 15).
- Group 2: 10% PV (Figure 16).
- Group 3: 10% PV (Figure 17).
- Group 4: 20% PV (Figure 18).

Results prove that optimum slug size was realized at a lower percentage of PV for oil wet Groups 2 and 3 when compared to the water wet Group 1. Lithology didn't influence slug size, optimum size of limestone oil wet group and dolomite oil wet group is the same, 10% PV. Group 3 and 4 are both oil-wet dolomite but the former has high permeability, and the latter contains low permeability plugs. Although the optimum slug size was realized at a higher % PV in Group 4 when compared

to Group 3, the cumulative recovery achieved by Group 4 low permeability plugs was slightly greater.

As discussed in Chapter 1, various literature agrees that LSW ability to alter an initially oil wet grain surface to a less oil wet state is what makes this technique recover more oil. Lack of need for significant wettability alteration in an initially water wet formation dissolves the need of LSW. Conducted experimental work agrees with literature, Tables 14 and 15 report the results of Low salinity flood in Limestone high permeability samples belonging to initially water wet environment and initially oil wet environment respectively. Comparison of cumulative recovery percentages displayed in column 9 clearly shows the following distinction; while RF for water wet samples ranged between 25-58%, oil wet samples' RF was much more significant ranging between 72-89%.

Carboxylic adsorption onto dolomite surfaces is stronger than on limestone surfaces, making LSW slug less efficient in altering the wettability of the core (Mahani et al., 2017; Nasralla et al., 2018). Thus, limestone is more reactive to the active ions in seawater responsible for wettability alteration. Reported data in Tables 15 and 16 show higher cumulative recovery in limestone samples (72-89%) in comparison to dolomite samples (14-26%) under the same initial wettability and permeability conditions (oil wet + high k).

Comparison between Tables 16 and 17, reveal comparable cumulative recovery achieved by flood in both high and low permeability oil wet dolomite plugs. However, data recorded proves that for the low permeability cores most of the oil was produced by the low salinity slug, production almost ceased beyond that point.

Limestone cores used in this study are pure (anhydrite free) with an average grain density of 2.68 g/cc, despite that, high oil recovery was observed especially in oil wet cores. Such results disagree with Austad et al. (2011) and Zahid et al. (2012) that reported no recovery improvement in anhydrite free samples.

Sample 6 in the Dolomite Oil-wet High permeability group displayed a curious trend in Figure 17. Although this sample shares a similar effective pore volume to liquid and permeability to liquid as other members of the group, it was an outlier. Porosity is linked to the amount of oil that could be introduced to the core through oil flooding and permeability is linked to the rate at which oil is displaced during water flooding, both of these parameters were comparable to samples 1, 17, 18. Table 12 records the secondary oil flood data, which shows that while other group members had a flood size ranging between 2.7-3.5\*PV, sample 6 was flooded only 1\*PV under the same time period (24 hours). This could be due to permeability impairment during primary oil flooding. Another possibility would be high fracture connectivity in this particular sample which results in high permeability difference between fracture and matrix; petrophysical analysis required to draw definite conclusion. As a result, sweep efficiency is expected to be low during waterflooding.

Interfacial tension of crude oil-water mixtures is a complex function of various parameters including water salinity, temperature and pressure, crude polar components, pH, etc. (Buckley & Tianguang, 2005). Salting in effect and polarization of the interface are the two main mechanisms that compete on interfacial behavior. They result in the following:

- Adsorption of asphaltene molecules to the interface.
- Dissociation of Naphthenic Acids (NA) in the aqueous solution.

- Diffusion of surface-active materials toward the interface and displacement, rearrangement, and detachment of adsorbed polar components at the interface (Mokhtari & Ayatollahi, 2019).

In the Asab brine-crude oil system (Figures 20 and 21), the accumulation of ions at the interface due to the high ionic strength of the high salinity brine reduces the adsorption of the polar components from the crude oil into the oil–brine interface; this hinders the formation of the asphaltenic film. There are no significant changes in IFT with time; mean IFT is 9.786 mN/m.

In the Low-salinity seawater-crude oil system (Figure 22 and 23), the accumulation of surface-active agents at the interface results in the descending trend of IFT before stabilization. Mean IFT is 4.099 mN/m.

Capillary Number ( $N_c$ ) is the ratio of viscous forces to capillary forces. Increasing  $N_c$  reduces residual oil saturation (ratio of remaining oil to total effective pore volume) and increases oil recovery (ratio of produced oil to original oil in place). High capillary force plays a major role in limiting the recovery efficiency by trapping oil phase within rock interstices or pores. This parameter depends on interfacial tension (fluid–fluid interactions) and contact angle (fluid–rock interactions). Comparative analysis performed between LSW-crude and FW-crude, revealed that IFT dropped from 9.786 mN/m to 4.099 mN/m by utilizing low salinity seawater. This change is not significant enough to make IFT the major contributor to the observed improved recovery.

Multicomponent Ionic Exchange (MIE) between brine containing Potential Determining Ions (PDI) and carbonates grain surface reduces the strength of the ionic bond holding oil molecules to rock (Lager et al., 2008). Sulphate ( $\text{SO}_4^{2-}$ ) acts as a catalytic agent, reducing the carbonate's surface



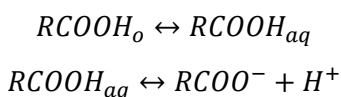
positive charge density by adsorbing to grain. The decrease in grain electrostatic repulsive forces results in the co-adsorption of Calcium ( $\text{Ca}^{2+}$ ). Reaction between  $\text{Ca}^{2+}$  and crude carboxylic groups breaks the attractive interactions between oil and grain, releasing adsorbed hydrocarbon and altering wettability to a more water wet state. This theory might explain the behavior of Group 2 as reported by Table 23. Calcium concentration decreased post flood from 13,840 ppm to 12,340 ppm. MIE is not valid for other carbonates groups in this study. Interestingly, Group 2 displayed the highest cumulative recovery in Table 15.

According to Hiorth et al. (2008), the lower concentration of Calcium ( $\text{Ca}^{2+}$ ) in the low salinity seawater slug causes Calcium Carbonates dissolution to restore equilibrium with the displacing phase. Calcite dissolution releases adsorbed crude polar components from grain surface and alters wettability to a more water wet state. This phenomenon was observed in Group 1 and 3 as reported by Table 23.

- Group 1: Calcium concentration increased from 13,840 ppm to 18,600 ppm.
- Group 3: Calcium concentration increased from 13,840 ppm to 14,720 ppm. Effect of designer water under ambient conditions is not as significant in dolomites when compared to limestone.

Table 23 records insignificant change in PDI content post IOR in Group 4, which contains the low permeability samples. This proves that LSW slug has minimal effect on this tight mineralogical group. Recovery observed in Table 17 under slug is possibility because of the experimental design that placed the slug flood first, meaning that the sample was going to release this oil volume regardless of water ionic concentration then cease to flow.

As the salinity of the flooding phase decreases, the concentration of crude oil naphthenic acids dissolved in the aqueous phase increases (Moradi et al., 2011). Naphthenic Acids (NA) are polar components that exist in crude oil and act as surface active materials. They stem from the heteroatoms present in the heavier components. NAs are hydrophilic, they adsorb at the interface and dissociate to produce carboxylic anions and hydrogen ions. Table 24 records how the release of hydrogen in the aqueous phase resulted in pH reduction in the effluent post IOR.



Future work should be instigated with an appropriate evaluation of crude oil composition, to quantify the amount of carboxylic material. According to Zhang and Sarma (2012) low salinity flood is more efficient with heavier oils when compared to lighter oils. Heavier oils have a higher initial oil wetness (polar components adsorb to grain surface), meaning that LSW slug has a higher chance to significantly alter wettability. Quantification of the amount of carboxylic material is achieved by measuring the acid number, work by Standnes and Austad (2000) revealed improved oil recovery and increased water wetness as the acid number decreases (carboxylic material increases).

Table 24: Post-IOR Average pH Readings

Group	ID	Mineralogy	pre-flood Wettability	k	pH			Avg
	FW				7.02	6.97	9.95	<b>8.0</b>
1	ZE1-8	limestone	water-wet	high	7.34	7.36	7.33	<b>7.3</b>
2	ZE1-2	limestone	oil-wet	high	7.35	7.33	7.32	<b>7.3</b>
3	ZE2-18	dolomite	oil-wet	high	7.34	7.35	7.32	<b>7.3</b>
4	ZE2-3	dolomite	oil-wet	low	7.43	7.44	7.41	<b>7.4</b>

Petrophysical analysis post flood in Table 25 revealed a reduction in sample ZE1-2 (Group 2) and ZE2-18 (Group 3) permeability. Fines migration is a mechanism initially proposed for LSWF in sandstone, but has been adopted by some researchers, such as Zahid et al. (2012) and Zhang and Sarma (2012), to describe recovery increase in carbonates. Released movable particles block some pore throats diverting fluid flow to upswept areas and increasing the microscopic sweep efficiency. Some researchers argue that this mechanism might be a more significant factor in improved oil recovery than wettability alteration (Lager et al., 2008).

Table 25 records that both the permeability of the representative samples from Group 1 and 4 increased. This increase was more dramatic in Group 4, which might be due to the formation of micro fractures during IOR process. This can explain how the low permeability group achieved comparable recovery to the high permeability group (refer to Tables 16 and 17). This proves that the recovery observed in Group 4 is due to mechanical process (micro-fractures) rather than chemical (wettability alteration).

Table 25: Change in Petrophysical Properties After IOR

		Pre-flood Flood		Post-flood Flood		Notes	
Group	Sample ID	Ø	k(g)	Ø	k(g)	Ø	k(g)
1	ZE1-8	20.5	11.6	15.2	13.1	decreased	increased
2	ZE1-2	18.7	17.1	16.5	6.5	decreased	decreased
3	ZE2-18	12.8	9.7	10.4	2.9	decreased	decreased
4	ZE2-3	10.2	4.1	13.5	18.7	increased	increased

Measurement of viscosity and density of crude produced revealed an increase when compared to original values (Table 26). This is due to the

formation of soft type emulsions (sodium naphthenates); dissociated naphthenic acids from crude oil react with sodium ions present in brine.

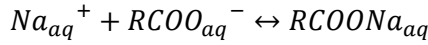


Table 26: Change in Crude Properties After IOR

	Pre-flood Flood	Post-flood Flood	Unit
API	0.8338	0.7713	°
Viscosity	7.1045	10.18	cp

Initial measurement of contact angle was conducted by saturating trim-ends with brine using vacuum and placing them in the denser phase (brine). Table 22 records contact angle values of representative trim-ends for the four groups and agrees with previously made conclusions based on primary oil flooding data; acquired plugs are initially highly water wet before aging. Final measurement of contact angle was recorded after aging trim ends, placing them in LSW for 24 hours and then transferring them to brine and awaiting oil droplet emergence.

Table 22 records the following:

- Group 1: Grain become more water wet after aging and IOR. Angle dropped from 50° to 36°.
- Group 2 and 3: No oil droplet. 24 hours was not long enough for chemical processes to take place and alter wettability to a more water wet state. Trim end is still strongly oil wet as a consequence of aging for 3 weeks.
- Group 4: No oil droplet. This is consistent with previous conclusions. LSW (chemical process) was not sufficient to improve oil recovery in low permeability dolomite samples.

It is important to note that past field applications of designer water in both secondary and tertiary mode have displayed improved oil recovery, however positive impact was not as high as the anticipated percentages observed from preparatory laboratory assessments (Singh & Sarma, 2021). Laboratory one dimensional core-floods are performed at low rates ( $<0.5$  cc/min), thus oil production is governed by capillary forces (combined effect of interfacial tension, pore throat size, and contact angle). Wettability alteration to a more water wet state by the LSW slug reduces the capillary end effect that strongly influence flow which positively impacts oil recovery (Derkani et al., 2018). Capillary force is not the dominant recovery factor under field applications which explains the overestimation of laboratory experiments' results.



# Chapter 4





## **Chapter 4: Conclusion**

### **4.1 Managerial Implication**

The energy industry today is facing great challenges because of the increasing demand from the prosperous more populous developing world. Limited availability and accessibility of non-renewable hydrocarbons, technical difficulty to recover higher percentages, and accountability to supply cleaner energy are few of the pressures encountered by the oil and gas industry. Thus, collaboration among industry and academia is crucial to meet the increasingly complex economic, technical, and environmental challenges. This thesis paper was written to share insights found through experimental investigations in hopes to contribute to the continual technical growth of the industry.

Improving the profitability and enhancing the sustainable potential of the industry depends on maximizing the crude oil output. Conventional techniques are capable to extracting only 30% of global oil reserves (Kokal & Al-Kaabi, 2010) which further highlights the importance of academic research and experimental investigations to successfully apply innovative techniques such as Low Salinity Slug Flood on field scale. According to Kokal and Al-Kaabi (2010), designer waterflooding can produce 10% more oil than conventional waterflooding. This equates 880 billion barrels of oil since Sheng (2013) suggested that improving global oil recovery by a factor of 1% has potential to yield 88 billion barrels of oil.

This thesis experiments on carbonate core plugs (Limestone & Dolomite), which is of substantial importance because 75% of the oil in the Middle East is found in carbonate fields (Akbar et al., 2001). Improved oil recovery techniques are essential in carbonates because of their oil-wet characteristics, large-scale heterogeneity, and presence of fractures which

result in complex fluid flow pathways and low oil recovery under simple waterflooding.

Performing IOR, recording results, and sharing them through this paper is important because the mechanism behind designer water is still not well defined in the industry. Inconsistent literature due to carbonate heterogeneity, high bonding energy between crude polar components and grain surface, and deficiency of clay makes this field in need of further experimental investigations.

#### **4.2 Research Implications**

Low salinity water flood in secondary mode introduces a slug of low salinity seawater at Swi, LSW disturbs initial thermodynamic equilibrium between rock-brine-crude interfaces facilitating a new equilibrium. This disturbance improves the wetting properties and increases the oil recovery. Significant parameters that were investigated in this research include:

- Wettability: Grain surface affinity towards one fluid over another.
- Contact angle: Quantifies wettability. Liquid wettability increases as the angle of the droplet on the solid decreases.
- Interfacial tension: Forces governing liquid-liquid interfaces.
- Recovery Factor: Ratio of produced oil to initial oil in place which is affected by the displacement mechanism. Purpose of flood is to maximize this parameter.

Significant comparisons made in this research were between four groups:

Group 1: Limestone, high permeability, aged in brine to introduce water wetness.

Group 2: Limestone, high permeability, aged in crude to introduce oil wetness.

Group 3: Dolomite, high permeability, aged in crude to introduce oil wetness.

Group 4: Dolomite, low permeability, aged in crude to introduce oil wetness.

This work yielded the following conclusions:

1. Wettability has a significant impact on the optimum slug size of low salinity water flooding.
2. Lithology has insignificant impact on the optimum slug size of LSW flooding of oil wet system.
3. Permeability effect on the optimum slug size cannot be described in simple terms as the pervious parameters and might require further investigation. Results revealed a lower optimum slug size and a lower cumulative oil yield as well for the high permeability plugs in oil wet system which implies that lower permeability sections of the reservoir will provide a higher contribution in terms of oil recovery than higher permeability zones.
4. In performing a reservoir simulation of low salinity flooding of a mixed wettability and heterogenous system, a comprehensive laboratory work is recommended using reservoir rock and fluid data to the determine optimum slug size and relative permeability data for various sections of the reservoir.
5. Future work must consider a larger sample size per study group for more comprehensive results. Time constraint and laboratory limitations constricted the size of the study and dictated use of representative samples for data analysis. Data analysis in future work must consider all subjects of study.

6. This study provides a rough estimate of the optimum slug size of a designer water process conducted on carbonate samples. Conclusions were made based on data collected from experimental procedure. Decisions were made taking into account project economics affected by seawater desalination expenses and environmental considerations of freshwater requirement along with oil yield, for example:
- Group 1: Optimum slug size is 30% PV because 40% PV yields only an additional 1% OIP.
  - Group 2: Optimum slug size is 10% PV, at this percentage production is maximized (90% OIP) whereas economics and environmental imprint are minimized.
  - Group 3: Optimum slug size is 10% PV, at this percentage production is maximized (15% PV) whereas economics and environmental imprint are minimized.
  - Group 4: Optimum slug size is 20% PV because 40% PV yields only an additional 5% OIP.

### **4.3 Future Endeavors**

Designer water is a complex area of study with broad possibilities for research and investigation. This research paper focused on: effect of lithology, permeability, and initial grain wettability introduced through aging on optimum slug size of low salinity water. However, the mechanisms at play during IOR introduce many curiosities which means this field of study has great potential for growth. Example of future endeavors that could be explored include:

- Dissolving surface-active cationic surfactants in low salinity seawater and investigating whether that will further enhance hydrocarbon recovery.

- Defining the dilution threshold of the prepared seawater. Dilution threshold is the value at which low salinity water slug yields the highest oil recovery value, beyond this value improvement in oil recovery ceases or decreases.
- Flooding dolomite samples at elevated temperatures to explore if that would increase oil recovery since observed cumulative recovery at the conclusion of flood under ambient temperature wasn't as significant as the values recorded for limestone samples. According to Mahani et al. (2017) wettability of dolomite surfaces improved substantially at high temperatures which resulted in contact angle reduction and wettability alteration from strongly oil wet to a more water wet condition.
- Exploring the increment of increase in oil recovery generated if mode of low salinity sea water was altered from slug flood of soak flood. In field, this would translate to injecting a certain PV size of LSW into the reservoir and closing the well for a certain period of time.
- This study considered recovery key parameters (injection water composition, grain wettability, immiscible fluids' interfacial tensions) to yield meaningful results. Future endeavor should consider field conditions (operational aspects, subsurface geological uncertainties, surface facilities) to make study more representative of real reservoir flood.

## References

- Akbar, M., Alghamdi, A. H., Carnegie, A., Dutta D., Olesen, J. R., Chourasiya, R. D., Logan D., Netherwood, R., Duffy, & Russell, S. (2001). A Snapshot of Carbonate Reservoir Evaluation. *Oilfield Review*, 12(4), 20-21.
- Al-Hadhrami, H. S., & Blunt, M. J. (2000). Thermally Induced Wettability Alteration to Improve Oil Recovery in Fractured Reservoirs. *SPE Res Eval & Eng*, 4(3), 179-186.
- Alhammadi, M., Mahzari, P., & Mehran, S. (2017). "Experimental Investigation of the Underlying Mechanism Behind Improved Oil Recovery by Low Salinity Water Injection in Carbonate Reservoir Rocks." Paper presented at the Abu Dhabi International Petroleum Exhibition & Conference, Abu Dhabi, UAE.  
<https://doi.org/10.2118/188352-MS>.
- Aljaberi, A., & Mehran, S. (2019) "A New Approach to Simulate Low Salinity Water Flooding in Carbonate Reservoir." Paper presented at the SPE Middle East Oil and Gas Show and Conference, Manama, Bahrain. <https://doi.org/10.2118/195081-MS>.
- Anderson, W. G. (1986). Wettability Literature Survey- Part 1: Rock/Oil/Brine Interactions and the Effects of Core Handling on Wettability. *J Pet Technol*, 38(10), 1125-1144.
- Austad, T., Shariatpanahi, S. F., Strand, S., Black, C. J., & Webb, K. J. (2011). Conditions for a Low-Salinity Enhanced Oil Recovery (EOR) Effect in Carbonate Oil Reservoirs. *Energy & Fuels*, 26(1), 569-575.
- Buckley, J. S., & Tianguang, F. (2005). Crude Oil/Brine Interfacial Tensions1. *Petrophysics*, 48(3). Retrieved 10th January 2022, from [https://www.researchgate.net/publication/254509032\\_Crude\\_OilBrine\\_Interfacial\\_Tensions1](https://www.researchgate.net/publication/254509032_Crude_OilBrine_Interfacial_Tensions1).
- Cuiec, L., Bourbiaux, B., & François, K. (1994). Oil Recovery by Imbibition in Low-Permeability Chalk. *SPE Form Eval*, 9(3), 200-208.

- Derkani, M., Fletcher, A., Abdallah, W., Sauerer, B., Anderson, J., & Zhang, Z. (2018). Low Salinity Waterflooding in Carbonate Reservoirs: Review of Interfacial Mechanisms. *Colloids and Interfaces*, 2(2), 200-208.
- Erke, S. I., Volokitin, Y. E., Edelman, I. Y., Karpan, V. M., Nasralla, R. A., Bondar, M. Y., Mikhaylenko, E. E., & Evseeva, M. (2016). "Low Salinity Flooding Trial at West Salym Field." Paper presented at the SPE Improved Oil Recovery Conference, Tulsa, Oklahoma, USA. <https://doi.org/10.2118/179629-MS>.
- Faramarzi-Palangar, M., Mirzaei-Paiaman, A., Ghoreishi, S. A., & Ghanbarian, B. (2021). Wettability of Carbonate Reservoir Rocks: A Comparative Analysis. *Applied Sciences*, 12(1). <https://doi.org/10.3390/app12010131>.
- Graue, A., Aspenes, E., Bognø, T., Moe, R. W., & Ramsdal, J. (2002). Alteration of Wettability and Wettability Heterogeneity. *Journal of Petroleum Science and Engineering*, 33(1-3), 3-17.
- Hiorth, A., Cathles, L., Kolnes, J., Vikane, O., Lohne, A., & Madland, M. (2008). "Chemical Modelling of Wettability Change In Carbonate Rocks." Paper presented at the 10th Wettability Conference, Abu Dhabi, UAE. Retrieved 5th February 2022, from [https://www.researchgate.net/publication/287139258\\_Chemical\\_modelling\\_of\\_wettability\\_change\\_in\\_carbonate\\_rocks](https://www.researchgate.net/publication/287139258_Chemical_modelling_of_wettability_change_in_carbonate_rocks).
- Kazankapov, N. (2014). Enhanced Oil Recovery in Caspian Carbonates with "Smart Water". Paper presented at SPE Russian Oil and Gas Exploration & Production Technical Conference and Exhibition. <https://doi.org/10.2118/171258-ru>.
- Kokal S., & Al-Kaabi, A. (2010). Enhanced Oil Recovery: Challenges & Opportunities. *World Pet Coun Off Publ.*, 12, 64-8.
- Kyte, J. R., Naumann, V. O., & Mattax, C. C. (1961). Effect of Reservoir Environment on Water-Oil Displacements. *J Pet Technol*, 13(6), 579-582.

- Lager, A., Webb, K. J., Black, C. J. J., Singleton, M. & Sorbie, K.S. (2008). "Low Salinity Oil Recovery - An Experimental Investigation." Paper presented at the International Symposium of the Society of Core Analysts, Trondheim, Norway. Retrieved 6th February 2022, from <http://www.jgmaas.com/SCA/2006/SCA2006-36.pdf>.
- Mahani, H., Menezes, R., Berg, S., Fadili, A., Nasralla, R., Voskov, D., & Joekar-Niasar, V. (2017). Insights Into the Impact of Temperature on the Wettability Alteration by Low Salinity in Carbonate Rocks. *Energy & Fuels*, 31(8), 7839-7853.
- Mahzari, P., & Sohrabi, M. (2015). "Impact of Micro-Dispersion Formation on Effectiveness of Low Salinity Waterflooding." Paper presented at IOR 2015 - 18th European Symposium on Improved Oil Recovery, Dresden, Germany. <https://doi.org/10.3997/2214-4609.201412103>.
- McGuire, P. L., Chatham, J. R., Paskvan, F. K., Sommer, D. M., & Carini, F. H. (2005). "Low Salinity Oil Recovery: An Exciting New EOR Opportunity for Alaska's North Slope." Paper presented at the SPE Western Regional Meeting, Irvine, California. <https://doi.org/10.2118/93903-MS>.
- Milner, J. (1996). *Improved Oil Recovery in Chalk-Spontaneous Imbibition Affected by Wettability, Rock Framework and Interfacial Tension*. PhD, University of Bergen, Norway. Retrieved 11th February 2022, from [https://urn.nb.no/URN:NBN:no-nb\\_digibok\\_2014051908202](https://urn.nb.no/URN:NBN:no-nb_digibok_2014051908202).
- Mokhtari, R., & Ayatollahi, S. (2019). Dissociation Of Polar Oil Components In Low Salinity Water And Its Impact On Crude Oil-Brine Interfacial Interactions And Physical Properties. *Pet. Sci.*, 16, 328-343.
- Moradi, M., Alvarado, V., & Huzurbazar, S. (2011). Effect of Salinity on Water in Crude Oil Emulsions: Evaluation through Drop-Size Distribution Proxy. *Energy & Fuels*, 25(1), 260-268.
- Morrow, N., & Buckley, J. (2011) Improved oil recovery by low-salinity water flooding. *Journal of Petroleum Technology*, 63, 106-112.



- Nasralla, R. A., Van Der Linde, H. A., Marcelis, F. H., Mahani, H., Masalmeh, S. K., Sergienko, E., Brussee, N. J., Pieterse, S. G., & Basu, S. (2018). Low salinity waterflooding for a carbonate reservoir experimental evaluation and Numerical Interpretation. *Journal of Petroleum Science and Engineering*, 164, 640-654.
- RezaeiDoust, A., Puntervold, T., Strand, S., & Austad, T. (2009). Smart Water as Wettability Modifier in Carbonate and Sandstone: A Discussion Of Similarities/Differences In The Chemical Mechanisms. *Energy & Fuels*, 23(9), 4479-4485.
- Salathiel, R. A. (1973). Oil recovery by surface film drainage in mixed-wettability rocks. *Journal of Petroleum Technology*, 25(10), 1216-1224.
- Saner, S., Asar, H., Okaygun, H., & Abdul, H. (1991). Wettability Study of Saudi Arabian Carbonate Reservoir Samples. *The Arabian J. for Sci. and Eng.*, 16(3), 357-371.
- Seccombe, J. C., Lager, A., Webb, K., Jerauld, G., & Esther F. (2008). "Improving Waterflood Recovery: LoSal™ EOR Field Evaluation." Paper presented at the SPE Symposium on Improved Oil Recovery, Tulsa, Oklahoma, USA. <https://doi.org/10.2118/113480-MS>.
- Sheng, J. (2013). Water Based EOR in Carbonates and Sandstones: New Chemical Understanding of the EOR-Potential Using "Smart Water". In J. Sheng (Eds.), *Enhanced Oil Recovery Field Case Studies* (pp. 301-335). Gulf Professional Publishing.
- Singh, N., & Sarma, H. K. (2021). "Successful in the Lab, Not as Effective in the Field? Uncertainties in the Field Observations of Low Salinity Water Flooding in Sandstone and Carbonate Reservoirs-A Critical Analysis." Paper presented at the SPE Western Regional Meeting, Virtual. <https://doi.org/10.2118/200803-MS>.
- Standnes, D. C., & Austad, T. (2000). Wettability alteration in Chalk. *Journal of Petroleum Science and Engineering*, 28(3), 111-121.

- Tang, G. Q., & Morrow, N. R. (1997). Salinity, Temperature, Oil Composition, And Oil Recovery by Waterflooding. *SPE Reservoir Engineering*, 12(04), 269-276.
- Tiab, D., & Donaldson, E. C. (2015). Wettability. In D. Tiab & E. C. Donaldson (Eds.), *Petrophysics: Theory and Practice of Measuring Reservoir Rock and Fluid Transport Properties* (4th ed., pp. 319-349). Elsevier.
- Tweheyo, M. T., Zhang, P., & Austad T. (2006). "The Effects of Temperature and Potential Determining Ions Present in Seawater on Oil Recovery from Fractured Carbonates." Paper presented at the SPE/DOE Symposium on Improved Oil Recovery, Tulsa, Oklahoma, USA. <https://doi.org/10.2118/99438-MS>.
- Webb, K. J., Black, C. J. J., & Al-Ajeel, H. (2003). "Low Salinity Oil Recovery - Log-Inject-Log." Paper presented at the Middle East Oil Show, Bahrain. <https://doi.org/10.2118/81460-MS>.
- Yousef, A. A., Al-Saleh, S., Al-Kaabi, A., & Al-Jawfi, M. (2011). Laboratory Investigation of The Impact Of Injection-Water Salinity And Ionic Content On Oil Recovery From Carbonate Reservoirs. *SPE Reservoir Evaluation & Engineering*, 14(05), 578-593.
- Zahid, A., Shapiro, A., & Arne S. (2012). "Experimental Studies of Low Salinity Water Flooding in Carbonate Reservoirs: A New Promising Approach." Paper presented at the SPE EOR Conference at Oil and Gas West Asia, Muscat, Oman. <https://doi.org/10.2118/155625-MS>.
- Zhang, P., Tweheyo, M. T., & Austad, T. (2006). Wettability Alteration and Improved Oil Recovery in Chalk: The Effect of Calcium in the Presence of Sulfate. *Energy & Fuels*, 20(5), 2056-2062.
- Zhang, Y., & Sarma, H. (2012). "Improving Waterflood Recovery Efficiency in Carbonate Reservoirs through Salinity Variations and Ionic Exchanges: A Promising Low-Cost "Smart-Waterflood" Approach." Paper presented at the Abu Dhabi International Petroleum Conference and Exhibition, Abu Dhabi, UAE. <https://doi.org/10.2118/161631-MS>.

## List of Publications

Al-Attar, H., Alshadafan, H., Al Kaabi, M., Al Hassani, A., & Al Mheiri, S. (2020). Integrated optimum design of hydraulic fracturing for tight hydrocarbon-bearing reservoirs. *Journal of Petroleum Exploration and Production Technology*, 10(8), 3347-3361.

The logo of the United Arab Emirates University (UAEU) is displayed in white text on a red rectangular background.

جامعة الإمارات العربية المتحدة  
United Arab Emirates University



## UAE UNIVERSITY MASTER THESIS NO. 2022: 42

This thesis project falls under improved oil recovery, specifically designer water flooding in secondary mode. Experimental work investigated effects of lithology, wettability, and permeability on the optimum slug size of diluted seawater. Conclusions were drawn based on constructed figures depicting cumulative recovery achieved by slug sizes varying between 10-40% of PV, measuring contact angle and IFT, studying changes in samples' petrophysical properties, as well as analyzing effluent (ionic concentration, pH, API).

**Hala Khaled Hasan Alshadafan** received her Master of Science in Petroleum Engineering from the Department of Chemical and Petroleum Engineering, College of Engineering at UAE University, UAE. She received her BSc from the College of Engineering, UAE University, UAE.

[www.uaeu.ac.ae](http://www.uaeu.ac.ae)